# CAPÍTOL 4. CONCLUSIONS

## 4. CONCLUSIONS

Dels diversos treballs realitzats i presentats en aquest memòria, destaquen les següents conclusions:

- S'han desenvolupat i caracteritzat diversos sistemes de membranes basats en el transportador N-hexadecil-L-hidroxiprolina, HHP: des de membranes líquides suportades (SLM), fins a diversos tipus de membranes polimèriques (ACM, CAM i membranes basades en CPS). Tots aquests sistemes han resultat aptes per al transport del fàrmac propranolol, i tres d'ells, SLM, CAM i CPS, han permès, en diferent grau, la separació enantioselectiva del fàrmac d'estudi.

De l'estudi del sistema d'SLM resulta que:

- El pH de la solució de càrrega determina el pas de propranolol a través de la membrana, així com la naturalesa d'aquest transport (enantioselectiu o no) .
- Cal una mínima quantitat de transportador en la membrana (que equival a tres vegades la quantitat d'analit en la solució de càrrega), per tal que es doni el transport enantioselectiu de propranolol.

Per altra banda, dels estudis amb membranes polimèriques ACM, CAM i basades en $CPS_A$, se'n deriva que:

- El pas de propranolol a través de les membranes depèn de la morfologia d'aquestes i de la presència de transportador (a la membrana), que actua facilitant el transport del fàrmac d'estudi.
- El grau de transport de propranolol a través de les membranes ve determinat no solament pel pH de la solució de càrrega, sinó també pel pH de la solució receptora, la concentració de transportador a l'interior de la membrana i la capa de difusió adjacent a la cara activa de la membrana. El grau de transport augmenta en disminuir el pH de la solució receptora ($3 < pH < 7$) i en minimitzar la capa de difusió (augment de l'agitació o del cabal de les solucions aquoses), i també, en menys grau, en augmentar la concentració de selector a la membrana.
- L'enantioselectivitat del fàrmac propranolol està condicionada per la concentració de transportador a la membrana i per la velocitat total del seu transport. Mentre en augmentar la concentració de transportador (per CAM: 50 ó $12 < A/C < 100$ ó 120; per membranes basades en CPS: $0\% < CPS_A < 25\%$), augmenta l'enantioselectivitat del procés, augmentant la velocitat total del transport, la selectivitat del procés disminueix.
- S'ha aconseguit immobilitzar l'agent transportador enantioselectiu HHP en membranes polimèriques per diferents mètodes. A mesura que la immobilització és més fixa (grau

d'unió entre polímer i transportador més gran), s'aconsegueixen millores en la reproductibilitat del sistema, cosa que produeix sistemes més fiables.

Per últim, i de manera més general, podem concloure que:

- Les condicions òptimes de treball, en termes de flux i selectivitat, comunes a tots els sistemes de membrana estudiats, són: una solució de càrrega ajustada a pH 8 i amb una concentració de 0,1 g/L de propranolol; una solució receptora ajustada a pH 7; un mode de funcionament continu; i una concentració elevada de transportador en la membrana (aquest valor varia segons el tipus de sistema de membranes i el tipus d'immobilització del transportador).
- El transport de propranolol a través dels diversos sistemes de membrana investigats té lloc mitjançant dos tipus de mecanismes diferents:
  (1) un mecanisme de transport facilitat acoblat a un contratransport de protons. Aquest mecanisme, segons si el transportador es troba lligat covalentment o no al polímer, pot dur-se a terme mitjançant salts consecutius entre molècules de transportador, o bé mitjançant la difusió a través de la membrana del complex del fàrmac amb el transportador. En ambdós casos té lloc la formació d'un parell iònic entre el propranolol i l'HHP; i
  (2) un mecanisme de transport no facilitat, que correspon a la difusió del propranolol a través de la membrana.
- L'enantiòmer S-propranolol és el que presenta una major afinitat pel selector HHP, i conseqüentment, es transporta més lentament que l'enantiòmer R, en el cas d'SLM, o més ràpidament, en el cas de les CAM i les membranes basades en CPS.

**ANNEX A**

SEPARATION SCIENCE AND TECHNOLOGY
Vol. 39, No. 2, pp. 431–447, 2004

# Characterization of a Supported Liquid Membrane Based System for the Enantioseparation of *SR*-Propranolol by *N*-Hexadecyl-L-hydroxyproline

**Tània Gumí, Manuel Valiente, and Cristina Palet***

Universitat Autònoma de Barcelona, Facultat de Ciències, Departament de Química, Bellaterra, Barcelona, Catalunya, Spain

## ABSTRACT

A supported liquid membrane (SLM) containing the chiral selector *N*-hexadecyl-L-hydroxyproline (HHP) was characterized for the enantioseparation of a $\beta$-blocking drug. *SR*-propranolol was the target racemic mixture to be resolved by the membrane separation system. The different affinity shown by the selected carrier, HHP, for the two propranolol enantiomers produced a discrimination of their transport through this SLM. We investigated the influence of various chemical parameters involved in that system, such as the acidity of feed and receiving phases,

*Correspondence: Cristina Palet, Universitat Autònoma de Barcelona, Facultat de Ciències, Departament de Química, 08193 Bellaterra, Barcelona, Catalunya, Spain; Fax: 34-93-5812379; E-mail: cristina.palet@uab.es.



DOI: 10.1081/SS-120027567 0149-6395 (Print); 1520-5754 (Online)

as well as the carrier concentration in the membrane. Valuable knowledge on the transport mechanisms within this system was thus attained.

*Key Words:* SLM; Enantioseparation; β-Blocking drugs; Characterization.

## INTRODUCTION

It is now well known that the human body can, in certain cases, differentiate between the enantiomers of a racemic drug[1] due to their different biological activity. In most cases, only one of the enantiomers carries out a useful and necessary activity, while no specific activity is undertaken by the other; consequently, it is removed by the human body as an impurity. In certain (fortunately infrequent) cases, the second enantiomer is even found to have negative effects on human health. Since the demonstration of such effects, pharmaceutical industries have been forced to develop methodologies for producing pure enantiomers to ensure the desired activity in the administration of drugs. In the case of *SR*-propranolol, a β-blocking drug used for treating some cardiovascular anomalies, the *S*-isomer shows far more blocking activity than the *R*-isomer.[2,3]

To date, most methods employed principally in the pharmaceutical industry to elucidate enantiopure compounds, such as stereoselective asymmetric synthesis, biotransformation, the chiral separation processes based on the enzymatic kinetic resolution technique or diastereomeric crystallisation, have been shown to have several drawbacks from an industrial point of view. Some of these are the requirement of a considerable number of different steps, with the corresponding by-products and a high energy consumption consequent to this to produce a reasonable amount of one optically pure enantiomer.[4–6] In the case of certain chromatographic separations, e.g., HPLC, they are even not applicable at an industrial scale.

Recently, other separation processes based on chiral stationary phases have increasingly gained attention at an industrial level, as both pure enantiomers can be obtained at the same time with far less difficulty.[7] Among such processes, membrane-mediated separation techniques are particularly promising, especially if we take into consideration the fact that they can be used in a continuous mode and that both the cost and related energy requirements are reasonably low.[4] In addition, most of the membrane processes are performed at room temperature, which makes them energy efficient. Of these processes, supported liquid membranes (SLM) have considerable potential, as only a very small amount of an expensive chiral carrier is needed to accomplish for resolution of the proposed enantiomer.[8]



MARCEL DEKKER, INC.
270 Madison Avenue, New York, New York 10016

Different enantioselective carriers have already been tested for the enantioseparation of *SR*-propranolol by using liquid membrane (LM) systems, such as *N*-n-alkyl-hydroxyprolines,[9] or dialkyl tartrate.[10] In both cases, the carrier is present in the membrane phase and selectively forms a complex with one of the enantiomers, which is transported across the membrane by an ion pairing mechanism.[5,9] These transport systems are driven by a proton gradient between both feed and receiving aqueous phases. However, with respect to the influence of certain chemical parameters involved in these enantioseparation membrane systems, there is still a lack of all the information required to fully comprehend the process and for its optimization.

In the present work, SLMs impregnated with an isopropyl myristate solution containing *N*-hexadecyl-L-hydroxyproline as carrier were applied for the enantioselective transport of *SR*-propranolol. A study on the influence of certain chemical parameters in the liquid membrane system was carried out to characterize the chemistry of the transport system and to attain a better assessment of the required enantioresolution.

## EXPERIMENTAL

### Chemicals

*R*-propranolol hydrochloride, *S*-propranolol hydrochloride, and racemic propranolol hydrochloride, all p.a. grade, were supplied by Sigma-Aldrich (Germany). *N*-Hexadecyl-L-hydroxyproline (HHP), isopropyl myristate (IPM), triethanolamine and hydroxypropyl-$\beta$-cyclodextrin (HP-$\beta$-CD), all p.a. grade, were also purchased from Sigma-Aldrich (Germany). Figure 1 shows the molecular structures of both the carrier, HHP, and our target analyte, *SR*-propranolol.

All other reagents used (such as acids and inorganic salts) were of analytical grade. Doubly distilled water was used for all aqueous solutions. Organic and aqueous solutions were presaturated with each other before use.

### Membrane System

The membrane cell configuration (Fig. 2) used for transport experiments (supplied by Prof. J. A. Jonsson, Lund University, Sweden) consists of two circular polytetrafluoroethylene (PTFE) blocks (diameter 120 mm and thickness 8 mm) with grooves arranged as an Archimedes' spiral (depth 0.25 mm, width 1.5 mm, and length 2.5 m, with a total volume of ca. 0.95 mL). Two aluminum blocks (thickness 6 mm) were placed on both sides of the



MARCEL DEKKER, INC.
270 Madison Avenue, New York, New York 10016

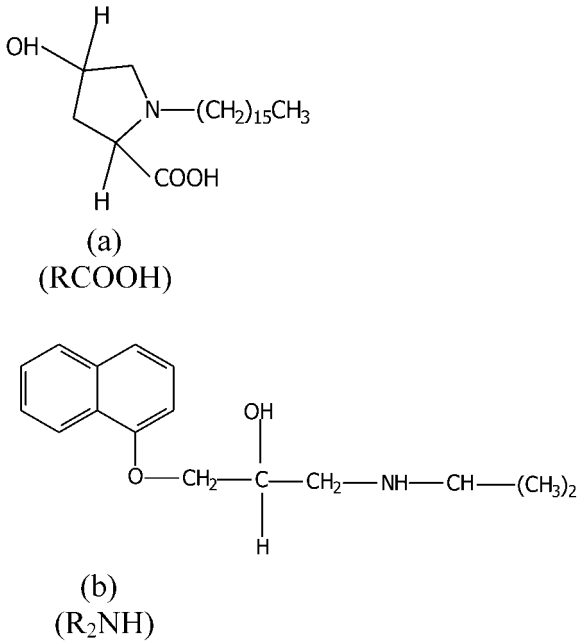


***Figure 1.*** Structures of (a) *N*-hexadecyl-L-hydroxyproline (HHP) and (b) propranolol.

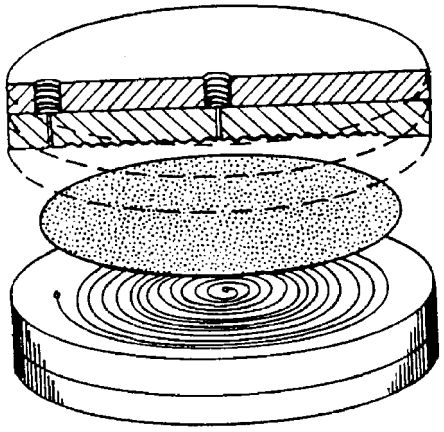

***Figure 2.*** Schematics of the membrane cell configuration used for the experiments.



MARCEL DEKKER, INC.
270 Madison Avenue, New York, New York 10016

PTFE blocks to stabilize the construction. Further details can be found elsewhere.[11,12] Porous polyvinylidenedifluoride (PVDF) membranes (Millipore GVHP, Millipore Corp., Germany), used as supports, were impregnated with a solution of HHP in IPM, by immersion of the solid polymeric support in the organic solution and sonication. In all the experiments, the amount of HHP in the membrane phase is expressed as the ratio of the quantity of HHP (in mols) in the membrane (taking into account the concentration of the HHP in the organic solution, and the effective volume of the porous support) to the amount of analyte (in mols) in the initial feed phase ($C/A$). The impregnated support is then placed between PTFE blocks and the whole construction is clamped tightly together with six screws. After installing the membrane and tubing, the excess solvent on the surface of the membrane was removed by passing doubly distilled water through both channels for 60 min, at 0.2 mL/min, which is the flux used for all the experiments. The total volume (20 mL) of each aqueous phase (both the feed and the receiving) was pumped with a peristaltic pump (Minipuls 3, Gilson, France) through acid-resistant tubing (Acid Manifold Tubing, Elkay Products, USA) connected to the membrane cell unit by screw plastic FIA fittings at both PTFE disks. Both aqueous phases were circulated throughout the whole experiment. The experiments started when both feed and receiving solutions entered the membrane cell. From that moment, samples of 0.5 mL were periodically withdrawn from the receiving phase channel, for about 5 h. In some cases, samples were also withdrawn after 20 h to confirm system behavior. A multimagnetic stirrer (A-03, SBS, Spain) was employed to stir both aqueous phases before entering the membrane cell unit, with the aim of supplying the membrane with homogeneous solutions. In all cases, the two solutions flowed in a counter-current mode. All experiments were performed at room temperature (24 $\pm$ 1°C).

## *SR*-Propranolol Determination

A capillary electrophoresis (CE) system (P/ACE SYSTEM MDQ, Beckman, USA) was used to analyze the concentration of both enantiomers in the collected samples. Determination was performed in 50-μm internal diameter, uncoated fused-silica capillaries of 60 cm (50 cm to the detector). Before each set of analyses, the capillary was rinsed with a 0.1 M NaOH solution, doubly distilled water, and finally, with the separation buffer solution. The latter consisted of 100 mM phosphoric acid adjusted at pH 4.4 with triethanolamine, containing 17.4 mM hydroxypropyl-$\beta$-cyclodextrin (HP-$\beta$-CD).[13,14] The applied voltage was 23 kV and UV detection was carried out at 210 nm. Samples were injected using the hydrodynamic mode for 5 s, at 0.3 psi. The capillary was thermostated at 20°C. Between



Marcel Dekker, Inc.
270 Madison Avenue, New York, New York 10016

consecutive determinations, the capillary was rinsed with doubly distilled water. At the end of the day, the capillary was washed with 0.1 M NaOH, doubly distilled water, and MeOH, which was used for removing organic material and for facilitating capillary drying.

## Parameters of Study

### Determination of the Extraction Efficiency

The extraction efficiency ($E$) is the parameter determined in all the experiments to quantify the *SR*-propranolol transport across the SLM.[11] It is defined as the portion of analyte extracted in the receiving phase from the total amount of analyte in the initial feed phase, as shown in Eq. (1).

$$E = \left[\frac{C_{\mathrm{r,i}} * V_{\mathrm{r,i}}}{C_{\mathrm{f,0}} * V_{\mathrm{f,0}}}\right] \tag{1}$$

where $C_{\mathrm{r,i}}$ is the concentration of analyte in the receiving phase at time i, determined as explained above, $V_{\mathrm{r,i}}$ is the volume collected from the receiving channel, $C_{\mathrm{f,0}}$ denotes the concentration of analyte in the initial feed phase, and $V_{\mathrm{f,0}}$ corresponds to the initial volume of feed solution. Extraction efficiency was determined for both *S*- and *R*- pure enantiomers and is labeled as *Es* or *Er*, respectively.

### Determination of the Enantiomeric Excess[15]

The enatiomeric excess (*ee*) is calculated from the previously obtained values of *Es* and *Er*, with the purpose of determining the enantioselectivity of the transport through the SLM system. The enantiomeric excess is defined as the ratio of the difference between the extraction efficiency of the two enantiomers to the total recovery of racemic analyte, within the receiving phase at time i:

$$ee = \left[\frac{Er_{\mathrm{i}} - Es_{\mathrm{i}}}{Er_{\mathrm{i}} + Es_{\mathrm{i}}}\right] * 100 \tag{2}$$

As seen from Eq. (2), a positive enantiomeric excess value will be obtained from a selective transport across the SLM of the *R*-enantiomer, and vice versa; negative *ee* will mean an enantioselective transport of *S*-enantiomer from the racemic mixture.



Marcel Dekker, Inc.
270 Madison Avenue, New York, New York 10016

## RESULTS AND DISCUSSION

An SLM impregnated with an isopropyl myristate solution containing HHP as carrier was applied to characterize the expected enantioselective transport of SR-propranolol. The influence of various chemical parameters was systematically investigated to determine their influence on *SR*-propranolol enantiomeric transport through SLM. For this purpose, the pH of both aqueous phases and the carrier concentration, which are usually determinant parameters in these chiral systems,[5] were separately varied and the influence of the presence of ionic species in both aqueous solutions was also checked. Finally, different operation modes were assayed and membrane stability was also checked.

### Influence of the Receiving Phase pH

Experiments with different pH in the receiving phase were carried out by using phosphate solutions at pH varying from 3 to 7. In all cases, the initial feed phase contained 0.05 g/L of racemate and was buffered with a borax solution at pH 8.[9] The carrier/analyte ($C/A$) ratio value was kept at about 1.4 throughout this set of experiments. Figure 3 shows experimental data

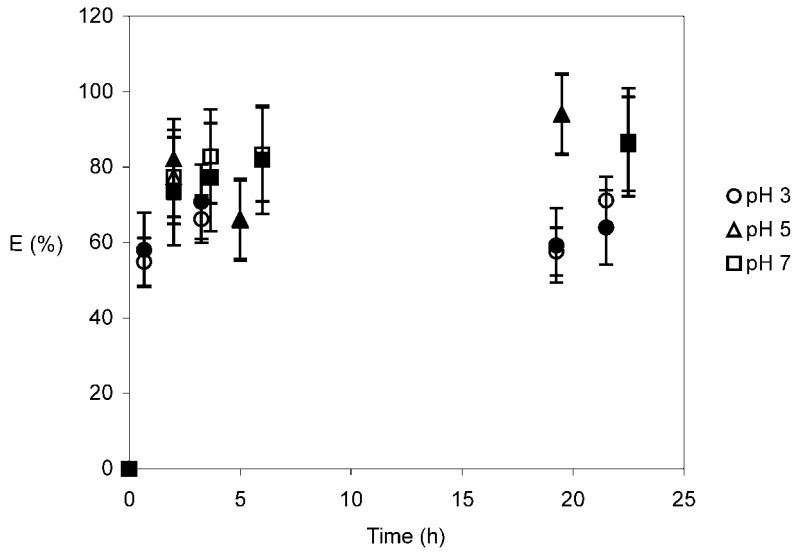


***Figure 3.*** Comparison of the extraction efficiency between different pH of the receiving phase. Empty and full symbol apply for the *R* and the *S* enantiomers, respectively. Bars indicate the standard deviation of the values.



MARCEL DEKKER, INC.
270 Madison Avenue, New York, New York 10016

expressed in terms of extraction efficiency ($E$) vs. time for each pH value investigated.

The high value of $E$ attained in all cases after approximately 20 h indicates an almost complete transport of the entire analyte from the feed to the receiving phase. This can be explained by two factors: on the one hand, by the concentration gradient of analyte between both aqueous phases, which favors analyte transport across SLM to the receiving phase;[2,16] on the other hand, the transport is also favored by the pH gradient between both aqueous phases, which enhances the analyte transport extent[17] and prevents its retro-extraction to the feed phase[2] (buffered at a higher pH). This behavior can be better understood by considering the two proposed transport mechanisms involved in this SLM system:[5,16] a nonfacilitated transport mechanism that takes place by diffusion and a facilitated transport mechanism that takes place by ion-pair complex formation between the analyte and the carrier (HHP), together with the corresponding proton antiport. Both mechanisms are schematized in Fig. 4. As seen in Fig. 3, the pH 7 of the receiving phase was sufficiently low to ensure a complete[17] analyte transport from the feed to the receiving phase, and for preventing the analyte from being retro-extracted, due to the higher amount of $H^+$ present in the receiving phase compared to the feed phase (buffered at pH 8). A receiving phase buffered with $Na_2HPO_4$ at pH 7 was, therefore, employed for all other experiments.

The uncertainty of the obtained values may be related to the low $C/A$ ratio used, which leads to higher relative errors in the impregnation step.

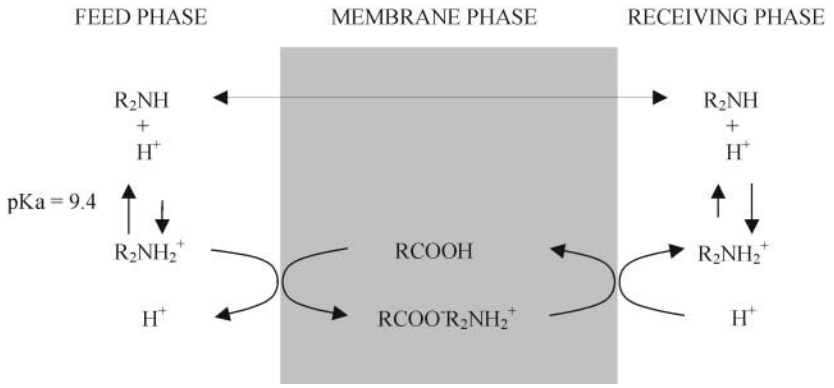


***Figure 4.*** Scheme of steps and mechanisms taking place in the membrane system. The carboxylic group of the carrier (RCOOH) has a pKa around 9.5.



MARCEL DEKKER, INC.
270 Madison Avenue, New York, New York 10016

### Influence of the Feed Phase pH

In this case, different solutions buffered at different pH (7 to 10) were assayed as feed phases. Initial analyte concentration in the feed phase was 0.05 g/L of racemate, and the $C/A$ ratio was maintained at 1.4. When investigating feed phase pH lower than 8, the corresponding receiving phase was lowered to pH 5 (instead of working at the optimum pH 7) to assure the necessary proton gradient between both aqueous phases. The results obtained are compared in Fig. 5.

The observed decrease of $E$ when the feed phase pH is decreased can be explained by considering the HHP and propranolol acid–base properties; the carboxylic group of the carrier HHP has a p$K$a of about 9.5[18,19] and the secondary amine of SR-propranolol has a p$K$a of about 9.4.[20] Therefore, at pH 7, the chemical equilibrium of the carrier HHP is notably shifted to its protonated form and the exchange of this proton by the cationic propranolol is not favored. The formation of the ion pair with the analyte (see Fig. 4) is then restricted, avoiding analyte transport across the membrane by the facilitated transport mechanism. On the other hand, the analyte is most probably present in its acidic form (positively charged) at this pH, so diffusion of the neutral form of propranolol through the membrane phase can hardly occur. For these reasons, a low $E$ is encountered and no selective transport is detected.

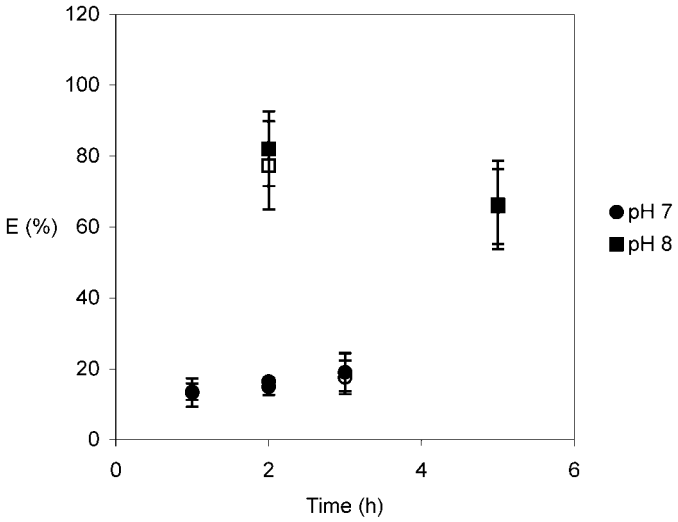


***Figure 5.*** Comparison of the extraction efficiency for different pH values of the feed phase. Empty and full symbol apply for the $R$ and the $S$ enantiomers, respectively. Bars indicate the standard deviation of the values.



Marcel Dekker, Inc.
270 Madison Avenue, New York, New York 10016

The feed phase pH was also varied from 8 to 10. In this set of experiments, initial feed phase contained 0.1 g/L of analyte, receiving phase pH was maintained at 7, and NaCl was used to equal the ionic strength between both aqueous phases. High *E* values were obtained in all cases. At these high pH conditions (feed pH of 9 to 10), propranolol is a neutral molecule ($R_2NH$). Thus, it will be able to diffuse easily through the SLM membrane leading to high E values (see Fig. 4), but it will not be capable of interacting with the carrier HHP. Selective transport is, therefore, not detected in such cases, as can be seen in Fig. 6.

Clear *ee* is obtained only when working with feed phase adjusted at pH 8. At this pH, despite HHP being mostly protonated, it may exchange its proton by the charged form of propranolol (the predominant form at this pH) more readily than at 7 feed phase pH, and may, therefore, participate in the ion-pair formation that is the base of the selective transport.

Disodiumhydrogen phosphate was occasionally used to buffer feed phase at pH 8, instead of borax, to investigate whether the nature of the buffer in any way influences the analyte transport across the designed SLM. Similar *E* values were encountered in both cases. This emphasizes the importance of the feed phase pH and also indicates that borax (the usual buffer employed) neither participates in any transport-limiting process nor does it work as a complexing agent for the *SR*-propranolol. Therefore, a feed phase buffered with $Na_2B_4O_7$ at pH 8 was used for all subsequent experiments.

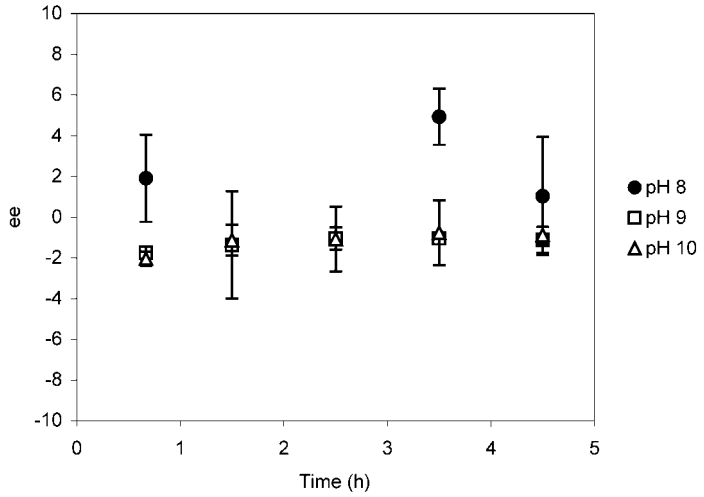


***Figure 6.*** Comparison of enantiomeric excess at different feed phase pH. Bars indicate the standard deviation of the values.



MARCEL DEKKER, INC.
270 Madison Avenue, New York, New York 10016

### Influence of the Analyte Concentration

The influence of the analyte concentration in the feed phase on the membrane transport was investigated. Differences in extraction efficiency ($E$) or in the enantiomeric excess (*ee*) were not detected when comparing a set of experiments performed with different initial analyte concentrations varying from 0.05 to 0.1 g/L. This may be due to the fact that, relatively speaking, both transport mechanisms involved in this system are fast enough not to be influenced by the amount of analyte that may mostly affect thermodynamic factors. Feed phases with 0.1 g/L of analyte were, therefore, prepared for all the following experiments, as high analyte concentrations led to improved analyte detection by CE.

### Influence of the Presence of Electrolytes in the Aqueous Solutions

To elucidate the chemical reactions involved in the membrane transport system, the role of proton and other cationic species was investigated. For that purpose, the influence of the presence of ionic species in the feed and receiving phases was evaluated by adding either NaCl or KCl to both phases and by maintaining all other parameters as previously indicated. No significant differences were observed between experiments with respect to the presence or absence of these electrolytes in the aqueous phases, when considering the variability of the data obtained corresponding to the uncertainty of the SLM system. In terms of *ee*, better performance of the SLM system was only detected when NaCl was added to the feed phase to balance the ionic strength on both sides of the membrane, with the aim of avoiding the effects of osmotic pressure.

We believe that the improvement in the *ee* that is observed in this case, by the comparison of Fig. 6 (pH 8) and Fig. 7 ($C/A = 1.4$), is due to a decrease in the resistance of the analyte against self-transport (especially in the case of facilitated transport) from the diluted to the more concentrated aqueous solution. This resistance is caused by the osmotic pressure phenomena previously referred to.[21]

### Influence of the Carrier Concentration in the Membrane Phase

To investigate the influence of the concentration of the carrier in the membrane phase, different experiments were performed by varying the



MARCEL DEKKER, INC.
270 Madison Avenue, New York, New York 10016

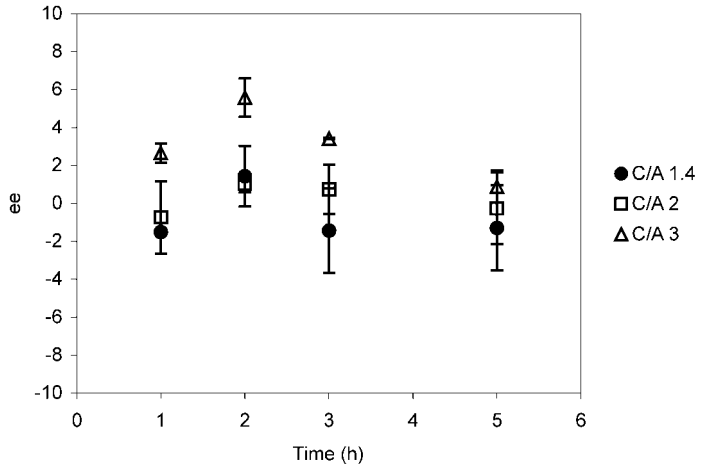


***Figure 7.*** Influence of the carrier concentration in the membrane, in terms of $C/A$ ratio, on the enantiomeric excess. Bars indicate the standard deviation of the values.

concentration of the HHP in the IPM organic solution, which impregnates the polymeric support. In each experiment, the feed phase, containing 0.1 g/L of analyte at pH 8, adjusted with borax buffer, and the receiving phase at pH 7, buffered with disodiumhydrogen phosphate, were pumped to the corresponding membrane side to determine the behavior of the SLM system. Experimental data are shown in Fig. 7 in terms of *ee* at the different carrier/analyte ($C/A$) ratio. $C/A$ ratios higher than 3 were limited by the relatively low solubility of HHP in IPM.

An enantioseparation increase is observed when increasing $C/A$ ratio; therefore, larger amounts of HHP enhance the contribution of the facilitated transport mechanism against the nonfacilitated mechanism. On the other hand, in the absence of a carrier, a similar diffusion of both enantiomers was detected.

Evidence of selective transport is obtained when a solution of HHP is impregnated in the membrane porous support. According to other research, the presence of secondary interactions (hydrogen bonding) in addition to ion pairing favors the affinity of the carrier for the *R*-enantiomer;[9] consequently, it is selectively transported to the receiving phase.

It is important to note that enantioseparation is only achieved during the first period of time in each experiment, corresponding to the period in which the facilitated transport mechanism occurs, up to the moment in which the difference in concentration of the two enantiomers within the aqueous phases of the SLM system is equaled by diffusion.[4,17] In the best case, when the $C/A$ ratio is 3, an *ee* of 5.6% is obtained 2 h after starting the experiment.



MARCEL DEKKER, INC.
270 Madison Avenue, New York, New York 10016

## Influence of the Mode of Operation

An assay in batch mode was carried out to investigate the influence of the operation mode on the extension of the transport and on its enantioselectivity. In this case, a feed phase containing 0.1 g/L of analyte, buffered with borax at pH 8, was pumped to both membrane sides for 2 h. The $C/A$ ratio value was 3.0. Subsequently, this solution was replaced by a receiving one, adjusted at pH 7, and was also pumped to both membrane sides. After 2 h, $E$ was measured. The results obtained are set out in Table 1 and are compared with the common continuous mode usually employed. That comparison makes clear the well-known advantages of the continuous mode, according to the extent of transport. The continuous mode, which has simultaneous extraction and reextraction mechanisms, permits the enhancement of transport extent by properly displacing the equilibriums involved in the SLM transport mechanism, making them efficient enough to be of promising potential at an industrial level. However, the operation mode shows no influence on the enantioselectivity of the transport under the tested conditions, as it is principally governed by the system's chemical parameters (pH of feed and receiving phases, and carrier concentration in the membrane).

## Membrane Stability

Separate experiments were carried out to evaluate the stability of the membrane by determining extraction efficiency, $E$, in successive experiments over a period of 14 days, using the same impregnated support. Initial feed phase was maintained as reported previously,[9] and the $C/A$ ratio value was 1.4 throughout all the experiments. Two samples were withdrawn from each experiment; the first of these after 1 to 2 h of starting the experiment, and the second sample just before terminating the experiment. To determine the stability of the SLM system, 16 experiments were carried out over 14 correlative days. Figure 8 shows the evolution of $E$ over time (in hours) for

***Table 1.*** Comparison of the extraction efficiency between experiments performed in continuous and batch operation modes.

| Experiment type | *Es* (%) | *Er* (%) |
|---|---|---|
| Continuous mode | 73.6 (30.4) | 78.4 (30) |
| Batch mode | 9.2 (1.2) | 9.6 (1.2) |

*Note:* Values in brackets represent the standard deviation of the data obtained.



Marcel Dekker, Inc.
270 Madison Avenue, New York, New York 10016

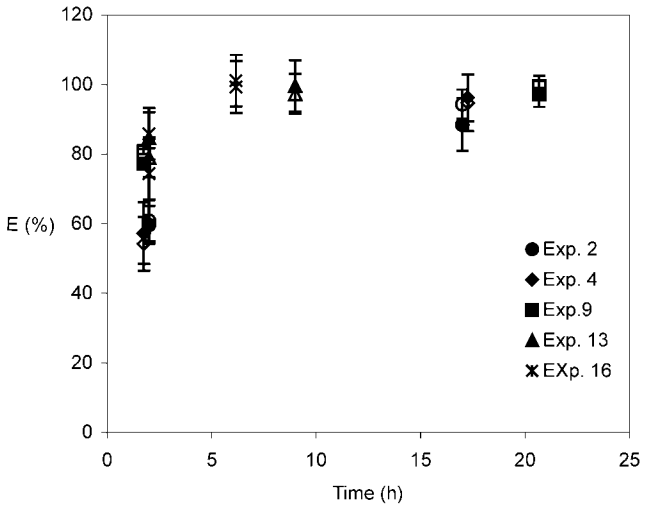


***Figure 8.*** Comparison of the extraction efficiency ($E$) for the different sequential experiment and time. Empty and full symbols apply for the $R$ and the $S$ enantiomers, respectively. Bars indicate the standard deviation of the values.

various experiments. No differences are observed between $E$ values obtained for all the experiments. After the last experiment, membrane appearance was still acceptable, as it presented some organic impregnation.

These results are very promising, taking into account the drawbacks and performance of SLM.[22,23] It may be a consequence of the organic solvent's good impregnating properties for the porous support used, together with the properties of the membrane cell configuration that minimize the leaching out of organic solution to the aqueous phases, and also supplementarily reduce the volatility of the organic solution. This makes the application of this system to semi-industrial levels genuinely attractive. Enantiomeric excess values show a high variability between experiments (but not a specific tendency) due to the fact that the $C/A$ ratio employed here was relatively low, as the principal focus of this study was to determine membrane lifetime.

## CONCLUSION

*SR*-propranolol enantioseparation was carried out through SLM system containing HHP as chiral selector. The system was characterized in terms of extraction efficiency ($E$) and enantiomeric excess ($ee$). The operation



MARCEL DEKKER, INC.
270 Madison Avenue, New York, New York 10016

conditions together with the chemical parameters of the feed and receiving phases were investigated.

Two of these studied parameters, namely the feed phase pH and the concentration of analyte within the membrane, have the greatest influence on the enantioseparation of the *SR*-propranolol racemic mixture. The pH of the feed phase governs the feasibility (or not) of the selective ionic-pair formation. The concentration of carrier in the membrane phase, when sufficiently high, facilitates the enantioseparation of the propranolol enantiomers across the SLM system. Additionally, good stability was encountered for the supported liquid membranes under study. A transport mechanism for the enantioseparation the *SR*-propranolol was then proposed.

## ACKNOWLEDGMENTS

This work was supported by C.I.C.Y.T. (Project ref: QUI99-0749-C01). T. Gumí acknowledges the predoctoral fellowship from the Departament d'Universitats, Recerca i Societat de la Informació de la Generalitat de Catalunya.

## REFERENCES

1. Krieg, H.M.; Bretenbach, J.C.; Keiser, K. Chiral resolution by $\beta$-cyclodextrin polymer-impregnated ceramic membranes. J. Membr. Sci. **2000**, *164*, 177–185.
2. Ahuja, S. Chiral separations and technology: an overview. In *Chiral Separations. Applications and Technology*; ACS: Washington, DC, USA, 1997; 1–7.
3. Coelhoso, I.M.; Cardoso, M.M.; Viegas, R.M.C.; Crespo, J.G. Modelling of transport mechanism in liquid membranes. In *Proceedings of Engineering with Membranes*, Granada, Spain, June 4–6, 2001; Luque, S., Alvarez, J.R., Eds.; Abs number VI; Universidad de Oviedo: Oviedo, 2001; 425–430.
4. Armstrong, D.W.; Jin, H.L. Enrichment of enantiomers and other isomers with aqueous liquid membranes containing cyclodextrin carriers. Anal. Chem. **1987**, *59*, 2237–2241.
5. Keurentjes, J.T.F.; Voermans, F.J.M. Membrane separations in the production of optically pure compounds. In *Chirality in Industry II. Developments in the Commercial Manufacture and Applications of Optically Active Compounds*; Wiley: Chichester, UK, 1997; 157–182.

6. Gao, Y.; Hanson, R.M.; Klunder, J.M.; Ko, S.Y.; Masamune, H.; Sharpless, K.B. Catalytic asymmetric epoxidation and kinetic resolution: modified procedures including in situ derivatization. J. Am. Chem. Soc. **1987**, *109*, 5765–5780.
7. Francotte, E.R. Enantioselective chromatography as a powerful alternative for the preparation of drug enantiomers. J. Chrom. A **2001**, *906*, 379–397.
8. Dzygiel, P.; Wieczorek, P.; Jonsson, J.A.; Milewska, M.; Kafarski, P. Separation of amino acid enantiomers using supported liquid membrane extraction with chiral phosphates and phosphonates. Tetrahedron **1999**, *55*, 9923–9932.
9. Heard, C.M.; Hadgraft, J.; Brain, K.R. Differential facilitated transfer across a solid-supported liquid membrane. Bioseparation **1994**, *4*, 111–116.
10. Keurentjes, J.T.F.; Nabuurs, L.J.W.M.; Vegter, E.A. Liquid membrane technology for the separation of racemic mixtures. J. Membr. Sci. **1996**, *113*, 351–360.
11. Calzado, J.A.; Palet, C.; Jonson, J.A.; Valiente, M. Metal affinity liquid membrane II. Facilitated transport of tryptophan. Anal. Chim. Acta **2000**, *417*, 159–167.
12. Wieczorek, P.; Jonsson, J.A.; Mathiasson, L. Concentration of amino acids using supported liquid membranes with di-2-ethylhexyl phosphoric acid as a carrier. Anal. Chim. Acta **1997**, *346*, 191–197.
13. Pak, C.; Marrito, P.J.; Carpenter, P.D.; Amiet, R.G. Enantiomeric separation of propranolol and selected metabolites by using capillary electrophoresis with hydroxypropyl-$\beta$-cyclodextrin as chiral selector. J. Chrom. A **1998**, *793*, 357–364.
14. Fillet, M.; Bechet, I.; Chiap, P.; Hubert, Ph.; Crommen, J. Enantiomeric purity determination of propranolol by cyclodextrin-modified capillary electrophoresis. J. Chrom. A **1995**, *717*, 203–209.
15. Calzado, J.A. Separació de compostos aniònics i neutres amb membranes de transport facilitat. In *Millores en la Selectivitat*; Universitat Autónoma de Barcelona: Bellaterra, Spain, 2001; Ph.D. Thesis.
16. Hadik, P.; Szabo, L.P.; Nagy, E. Chiral separation with hollow-fiber membrane. In *Program and Abstracts*, Euromembrane 2000: Israel, September 24–27, 2000; 388.
17. Pirkle, W.H.; Bowen, W.E. Preparative separation of enantiomers using hollow-fiber membrane technology. Tetrahedron: Assymmetr. **1994**, *5* (5), 773–776.
18. Martell, A.E. Ed. *Stability Constants of Metal-Ion Complexes. Section II: Organic Ligands*, The Chemical Society: London, UK, 1964.



MARCEL DEKKER, INC.
270 Madison Avenue, New York, New York 10016

19. Dean, J.A. *Lange's Handbook of Chemistry*, Revised 10th Ed.; McGraw-Hill: USA, 1973.
20. Yarabe, H.H.; Billiot, E.; Warner, I.M. Enantiomeric separations by use of polymeric surfactant electrokinetic chromatography. J. Chrom. A **2000**, *875*, 179–206.
21. Garcia-Valls, R. New materials for lanthanids separation techniques. In *Activated Polymeric Membranes and Inorganic Materials for Chromatography*; Universitat Autónoma de Barcelona: Bellaterra, Spain, 1995; Ph.D. Thesis.
22. Neplenbroek, A.M.; Bargeman, D.; Smolders, C.A. Supported liquid membranes: stabilization by gelation. J. Membr. Sci. **1992**, *67*, 149–165.
23. Kemperman, A.J.B.; Bargeman, D.; Van den Boomgaard, Th.; Strathmann, H. Stabilization of supported liquid membranes by gelation with PVC. J. Appl. Polym. Sci. **1997**, *65* (6), 1205–1216.

Received January 2003
Revised April 2003



MARCEL DEKKER, INC.
270 Madison Avenue, New York, New York 10016

**ANNEX B**

ELSEVIER

Journal of Membrane Science 212 (2003) 123–134

journal of MEMBRANE SCIENCE

www.elsevier.com/locate/memsci

# Characterization of activated composite membranes by solute transport, contact angle measurement, AFM and ESR

T. Gumí [a], M. Valiente [a], K.C. Khulbe [b], C. Palet [a,*], T. Matsuura [b]

[a] *Grup de Tècniques de Separació en Química (GTS), Departament de Química, Universitat Autònoma de Barcelona, Bellaterra, Catalunya 08193, Spain*

[b] *Department of Chemical Engineering, Industrial Membrane Research Institute, University of Ottawa, Ottawa, Ont., Canada K1N6N5*

Received 20 June 2002; received in revised form 7 October 2002; accepted 8 October 2002

**Abstract**

In this article, various characterization techniques are used to determine the structural membrane properties of various activated composite membranes (ACMs), which have been developed in the last years in our laboratories of the *Universitat Autònoma de Barcelona (UAB)*. The mentioned ACMs were developed in an attempt to enhance the stability and lifetime of the well-known selective liquid membranes, for their application on selective transport of heavy metals and organic species, such as chiral compounds. Four different characterization techniques have been investigated with the aim to reach an actual microscopic information of the ACMs, and in that way, ascertain their future applications, by modifying their preparation methodology when needed. The characterization techniques here employed are: solute transport, contact angle measurement, atomic force microscopy (AFM) and electron spin resonance (ESR). The simultaneous employment of these techniques provide evidence of the presence, dimension and distribution of pores in membrane surface, as well as useful information about its hydrophilic properties, and confirmation of the immobilization of selective carriers into the membrane.

Actual values of pores size and distribution on the membrane surfaces were reached by comparison of the different techniques, and the presence of the selective transport agents checked was detected.


*Keywords:* Activated composite membranes; Solute transport; Contact angle measurement; AFM; ESR

## 1. Introduction

Selective liquid membranes have been successfully developed for the separation of metals, organic compounds and other species from bulk solutions [1–3]. The selective separation of these membranes is accomplished by the presence of selective compounds, called carriers, in the membrane phase. The carriers are responsible to facilitate the transport of the target component across the selective membrane. However, when tested under industrial separation conditions, these liquid membranes showed low stability and short lifetime [4,5]. In an attempt to improve the stability and the lifetime of the liquid membranes, activated composite membranes (ACMs) have been developed at the *Universitat Autònoma de Barcelona* laboratories, and applied successfully for various separation systems [6–8].

It is fundamentally very important to know the structure–performance relationship for the membrane to achieve any progress in membrane technologies [9,10]. Therefore, a detailed characterization of ACMs

* Corresponding author. Tel.: +34-935813475; fax: +34-935812379.
*E-mail address:* cristina.palet@uab.es (C. Palet).

0376-7388/02/$ – see front matter 
PII: S0376-7388(02)00490-8

**Nomenclature**

| | |
|---|---|
| $a$, $b$ | peak heights in the ESR spectrum (arbitrary units) |
| $C_f$ | solute concentration in the feed solution (ppm) |
| $C_p$ | solute concentration in the permeate (ppm) |
| $d_{max}$ | maximum pore size (nm) |
| $d_{min}$ | minimum pore size (nm) |
| $d_s$ | solute diameter (nm) |
| $f$ | solute separation (%) |
| $f(x, y)$ | surface relative to the center plane |
| $f_i$ | fraction of pores with diameter $d_i$ |
| $j$ | order number of pore when arranged in ascending order |
| $J$ | solvent flux through all the pores ($m^3/m^2$ s) |
| $L_x$, $L_y$ | dimensions of the surface $f(x, y)$ (nm) |
| $M$ | molecular weight (g/mol) |
| $n$ | number of pores measured from AFM images |
| $N$ | number of pores per unit area (pores/$m^2$) |
| $r$ | coefficient of correlation |
| $R_a$ | mean roughness (nm) |
| $S_p$ | surface porosity (%) |

*Greek letters*

| | |
|---|---|
| $\delta$ | skin layer thickness (μm) |
| $\eta$ | solvent viscosity (N s/$m^2$) |
| $\mu_p$ | mean pore size (nm) |
| $\sigma_p$ | geometric S.D. (nm) |
| $\Delta P$ | pressure difference across the pores/membrane (kPa) |

is required in order to extend their applications into the current emerging industrial needs such as the separation of chiral compounds.

A large number of different membrane characterization techniques have been investigated in the last decades, but none can give any decisive information when they are used individually. The best results are generally obtained by using various techniques simultaneously and by comparing their results. In this work, four characterization methods, i.e. the method based on the solute transport, the contact angle measurement, the atomic force microscopy (AFM) and the electron spin resonance (ESR), were investigated thoroughly to characterize several ACMs.

In order to predict the membrane performance, it is often necessary to know the mean pore size and the pore size distribution at the membrane surface [11]. Hence, several techniques, including various microscopic methods and a method based on the solute transport, have been attempted to determine these parameters [12]. Furthermore, in such attempt, it was found that the pore size distribution fitted to a log-normal distribution very well [13].

The atomic force microscopy (AFM), developed by Binnig et al. [14], allows the imaging of non-conducting samples, both in air and in liquid media, down to nanometer scale [11,15]. Its main advantage over the electron microscopic technique is that no sample pre-treatment is required. Although relatively novel, its application to the study of synthetic membranes has grown very fast during the past few years [16]. From the AFM images of membrane surfaces, various morphological parameters can be obtained including mean roughness and root mean square of Z data [11].

The electron spin resonance (ESR) is nowadays a well-established technique, as a method to characterize synthetic membranes. This method allows to study the structure of synthetic membranes by analyzing the ESR signals from an ESR spin probe that is incorporated into the membrane, since the signal depends on the environment of the spin probe [17].

While the above methods are useful for the morphological characterization of synthetic membranes, the characterization based on the contact angle measurement provides information on the hydrophilicity and hydrophobicity of the membrane surface. The hydrophilicity/hydrophobicity characteristics of the membrane surface are expected to govern the surface wettability by liquids, especially by water, and subsequently govern the membrane performance in various applications [18]. There are three methods to measure contact angles, which are; the captive bubble, the Wilhelmy plate technique and the sessile drop, which has been used in this work [19].

In the present work, various ACMs containing different carriers are characterized and relevant information, regarding the incorporation of the carriers into the membranes is obtained. One of the

studied carriers is 2-(di-ethyl-hexyl) phosphoric acid (Dehpa), which is widely employed for the facilitated transport of metals [7]. Other two carriers used are selective chiral transport agents, such as Nopol and *N*-hexadecyl-L-hydroxy proline (Hhp). As indicated, four different characterization techniques, including the method based on the solute transport, the contact angle measurement, the AFM, and the ESR are used.

## 2. Theory

### *2.1. Evaluation of the membrane surface parameters (mean pore size, geometric S.D., molecular weight cut-off (MWCO), pore density and surface porosity)*

The pore size and pore size distribution of the membranes were determined based on the separation data obtained from ultrafiltration experiments using polyethylene glycol (PEG) and polyethylene oxide (PEO) of different molecular weights, as solutes. The solute separation is defined as:

$$f = \left(1 - \frac{C_p}{C_f}\right) \times 100 \tag{1}$$

where $C_p$ and $C_f$ are the solute concentrations in the permeate and in the bulk of the feed solution. In order to determine the membrane surface parameters the solute separation data were transferred on a log-normal probability plot of solute separation $f$ versus the solute diameter $d_s$. The latest was obtained from the Einstein–Stokes radius (ESr) of the solute. From this log-normal probability plot, MWCO is obtained from the solute diameter at $f = 90\%$, mean pore size $\mu_p$ can be calculated as the solute diameter that corresponds to $f = 50\%$, and the geometric S.D., $\sigma_p$ can be obtained from the ratio of solute diameter at $f = 84.13$ and at 50%.

The molecular weight of PEG and PEO, $M$ was converted to the ESr from the empirical equations [11,20–23]:

$$\mathrm{ESr} = 16.73 \times 10^{-10}\, M^{0.557} \tag{2}$$

for PEG and

$$\mathrm{ESr} = 10.44 \times 10^{-10}\, M^{0.587} \tag{3}$$

for PEO, respectively.

From the mean pore size and the geometric S.D., the pore size distribution of the membrane can be obtained as the cumulative distribution function and the probability density function [24].

Surface porosity $S_p$, defined as the ratio between the area of pores to the total membrane surface area [11], was calculated using the equation:

$$S_p = \frac{N\pi}{4}\left(\sum_{d_{min}}^{d_{max}} f_i d_i^2\right) \times 100 \tag{4}$$

where $N$ is the total number of pores per unit area (pore density) and $f_i$ the fraction of the number of pores with diameter $d_i$. $N$ was determined using the following equation:

$$N = \frac{128\eta\delta J}{\pi\,\Delta P \sum_{d_{min}}^{d_{max}} f_i d_i^4} \tag{5}$$

where $\delta$ is the length of pores and considered to be equal to the thickness of the top polyamide layer, $\eta$ the solvent viscosity, $\Delta P$ the pressure difference across the pores and $J$ the solvent flux. One micrometer was used for $\delta$, according to the thickness obtained for the polyamide layer, by using the impedance spectroscopy method, in an earlier work [25].

### *2.2. Analysis of the surface image obtained by AFM*

The nodule and the pore sizes were measured by visual inspection of their line profiles from various AFM images corresponding to different parts of the same membrane.

In order to determine the mean pore size of the membranes, from the AFM images, the measured pore sizes were arranged in ascending order and were assigned the corresponding median rank, that is calculated from the following formula [11,26]:

$$\text{Median rank} = \frac{j - 0.3}{n + 0.4} \times 100 \tag{6}$$

where $j$ is the order position of the pore size and $n$ the total number of pores measured. To obtain a cumulative distribution function graph, these median ranks are plotted on the ordinate against pore sizes, arranged in an increasing order on the abscissa. This plot will yield a straight line on a log-normal probability paper if the

pore sizes have a log-normal distribution. From this graph, the mean pore size, $\mu_p$, and the geometric S.D., $\sigma_p$, can be calculated, as reported previously [11].

To determine the pore density of the membranes, the number of pores was counted visually from several AFM images covering an area of ca. 200 nm × 200 nm. On the other hand, the porosity of the surface, $S_p$ was calculated by using the Eq. (4) [11].

The differences in the membrane surface morphology can be expressed in terms of various roughness parameters, all of them measurable by the AFM technique. The mean roughness $R_a$ which is obtained from the following formula [11]:

$$R_a = \frac{1}{L_x L_y} \int_0^{L_x} \int_0^{L_y} |f(x, y)| \, dx \, dy \quad (7)$$

corresponds to the mean value of surface relative to the center plane, this is the plane for which the volume enclosed by the image above and below this plane is equal [11]. Several AFM images (of ca. 1000 nm × 1000 nm) of different parts of the membrane were analyzed properly in order to obtain the $R_a$ parameter.

## 3. Experimental

### 3.1. Materials

Non-woven fabric was used as a mechanical support (backing material) for the membranes. Polysulfone Udel (P-3500) from ICI (UK) and *N*,*N*-dimethylformamide (DMF) (Fluka, Switzerland) were used for the preparation of the porous membrane layer. 1,3-Phenilenediamine (Merck, Germany), trimesoyl chloride (Sigma–Aldrich, Germany) and hexane (Sigma–Aldrich, Germany) were used for the preparation of top membrane layer. 2-(Di-ethyl-hexyl) phosphoric acid (Dehpa) (Sigma–Aldrich, Germany), Nopol (Fluka, Switzerland) and *N*-hexadecyl-L-hydroxyproline (Hhp) (Sigma–Aldrich, Germany) were used as carriers. Polyethylene glycol (PEG, *M* up to 35,000 g/mol), polyethylene oxide (PEO, *M* up to 400,000 g/mol), supplied either by Aldrich (USA) or Fluka Chemika (Switzerland), sodium chloride (Anachemia, Canada) and magnesium sulfate (Sigma, USA) were used as solutes in ultrafiltration experiments. 2,2,6,6-Tetramethyl-1-piperridinyloxy-free radical, namely Tempo (from Sigma–Aldrich, USA) was used as spin probe for the ESR experiments. All reagents employed were of analytical grade.

### 3.2. Membrane preparation

Polysulfone was dissolved in DMF to a concentration of 15 wt.% and the solution was cast on the surface of the non-woven fabric and, all together, immersed into a gelation bath. Then, a thin polyamide layer was formed, on the top surface of the polysulfone membrane, by reacting, in situ, 1,3-phenylenediamine dissolved in water with trimesoyl chloride dissolved in hexane. The membranes were activated by adding one of the selected carriers, into the hexane solution used for the in situ interfacial polymerization of the top polyamide layer. More details of the membrane preparation are given elsewhere [7,27]. One of the membranes was used as a blank without incorporating any carrier. The membranes are labeled, hereafter, as Mblank, Mdehpa, Mnopol and Mhhp. Mblank corresponds to the blank membrane, while the abbreviated names of the carriers are included in the codes of the last three membranes.

### 3.3. Solute transport by ultrafiltration experiments

The ultrafiltration experiments were performed, by using the continuous membrane test cells, each having an effective membrane area of 13.85 $cm^2$. Three cells were connected in series. All the experiments were conducted at 25–26 °C, and at 344.7 kPa gauge (50 psig). The details of the experimental procedure are given elsewhere [28].

Pure water permeation (PWP) flux was measured for each membrane by circulating distilled water through the membrane system before starting the corresponding solute transport experiment. Polyethylene glycol (PEG) and polyethylene oxide (PEO) were used as the solutes in the feed solutions for the ultrafiltration experiments. The initial feed concentration was 200 ppm. PEG/PEO separation experiments were conducted starting from the lower molecular weight solute. The system was thoroughly flushed with distilled water between runs made with PEG/PEO solutes of different molecular weights. PEG/PEO contents in the feed and in the permeate solutions were determined from the amount of total organic carbon

(TOC) measured by using a Total Organic Carbon Analyzer (Dohrmann DC-190, Folio Instruments Inc.).

The separation of NaCl and $MgSO_4$ was conducted at the same conditions as the above ultrafiltration experiments. The experimental procedure is also the same as the one already described. In this case, the concentration of the electrolytes both in the feed and the permeate solutions was determined by conductivity method using a CDM 80 conductivity meter (Radiometer, Copenhagen).

The solute separation was calculated in both cases by using Eq. (1).

### 3.4. Contact angle measurement

The sessile drop method was used to measure the contact angle of the prepared membranes [19]. A 6-$nm^3$ droplet of distilled water was placed on the membrane surface by means of a 0.10 ml (Gastight, Hamilton Co., Nevada, USA) syringe and contact angle was measured by a horizontal beam comparator (Scherr-Tumico, 22-2000 Series, Model 20-4200, St. James, Minnesota, USA). Advancing contact angle measurement was followed by receding contact angle measurement, wherein the volume of the initially added droplet is either increased or decreased, respectively, depending on the angle to be measured, until the three-phase boundary moves over the solid surface [19]. The contact angle hysteresis was calculated as the difference of these two contact angles. The capillary pipette end of the micro-syringe was kept immersed into the drop during the entire period of measurement in order to avoid vibration and distortion of the droplet during the volume change [19].

### 3.5. Atomic force microscopy

AFM images were obtained by using Nano Scope III equipped with a 1553D scanner from Digital Instruments, USA. The speed of scanning was 2.98 Hz. Tapping mode of AFM in air was used to investigate the membrane surface morphology. Silicone nitride cantilevers were employed.

### 3.6. Electron spin resonance

ESR measurements were made with an x-band Bruker 200 DC spectrometer (Germany). The membrane sample (with area of 0.5 $cm^2$) was fixed in the tissue cell supplied by Willmad Glass N.J. (USA). All measurements were performed at $24 \pm 1\,^{\circ}C$. Before measurement, membranes were soaked in aqueous Tempo (0.01%) solution for 1h. Afterwards, the membranes were rinsed with distilled water to remove the last traces of Tempo solution from the membrane surfaces. Excess of water from the membrane surfaces was removed by pressing the wet membrane between two filter papers.

## 4. Results and discussion

### 4.1. Membrane characterization based on solute transport

Fig. 1 shows the log-normal probability plot of PEG/PEO separation data versus solute diameter for all the studied membranes. The linear correlation found between these parameters (with correlation coefficients >0.9) indicates that the log-normal distribution is quite appropriate to describe the pore size distribution in the blank membrane and also in the ACMs. Some characterization parameters pertinent to the Mblank membrane and the three ACMs are given in Table 1. From these experiments we may affirm that:

(a) ACMs are workable under the pressure at which the ultrafiltration experiments were carried out; i.e. at 50 psig;
(b) the mean pore size values encountered for the four membranes (3.75–10.75 nm), correspond to pore size values of the shiny surface of polysulfone films of ultrafiltration membranes [29], although a thin polyamide layer was cast on the top of the porous sublayer;

Table 1
Some membrane surface characterization parameters obtained by the method based on solute transport

| Membrane | $\mu_p$ (nm) | $\sigma_p$ (nm) | MWCO (kg/mol) | $N$ (pores/$\mu m^2$) | $S_p$ (%) |
|---|---|---|---|---|---|
| Mblank | 10.75 | 2.48 | 304.3 | 5.99 | 0.15 |
| Mdehpa | 8.10 | 2.55 | 198.2 | 2.18 | 0.03 |
| Mnopol | 5.69 | 2.60 | 113.8 | 7.28 | 0.08 |
| Mhhp | 3.75 | 2.57 | 54.3 | 11.41 | 0.08 |

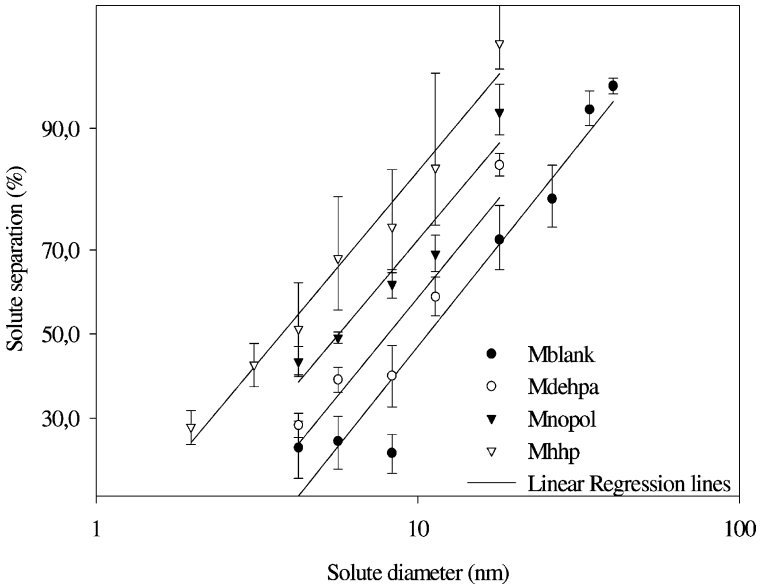


Fig. 1. Solute separation versus solute diameter for the four composite membranes (error bars correspond to S.D.).

(c) the surface porosity of Mblank membrane (0.15%) is two orders of magnitude lower than those of ultrafiltration membranes of a similar mean pore size, since the porosity of the latter membranes is reported to be 7–12% [29]. This means that the pores are considered as defects of the evenly coated polyamide layer;
(d) the surface porosity values of ACMs are even smaller than that of Mblank; and
(e) the mean pore size of Mblank membrane is greater than the ACMs. This means that the incorporation of the carriers decreased the mean pore size. It is probably because the carrier stays in the pore and thus partially blocks the flow of water through the pores. The difference in the pore size within the ACMs is probably due to the difference in compatibility of the carriers with the substrate membrane.

Also, we see from Table 1, that the geometric S.D. are almost constants and similar to the values of other synthetic membranes [11]. The data on MWCO parallels those of the mean pore size, as expected. The cumulative pore size distribution and the probability density function curves were generated based on the mean pore size and the geometric S.D. values, to finally calculate the pore density and the surface porosity reported in Table 1.

On another hand, the PWP flux data determined are given in Fig. 2. Mblank and Mhhp membranes showed the maximum and minimum PWP flux, respectively, corresponding to the largest and the smallest mean pore size.

The collected data corresponding to the separation of electrolyte solutes are shown in Table 2. The solute separations were generally low, partially due to the low operating pressure (50 psig) used in these experiments [28]. Although the electric charges are present in the membrane [29,30], they did not contribute greatly to the rejection of the electrolyte solutes. However, the Mblank membrane appeared to have higher separation values than the rest of the

Table 2
Separation data collected from ultrafiltration experiments for the four composite membranes, by using electrolyte solutes

| Membrane | $f_{NaCl}$ (%) | $f_{MgSO_4}$ (%) |
|---|---|---|
| Mblank | 27 ± 18 | 26 ± 13 |
| Mdehpa | 10 ± 4 | 8 ± 2 |
| Mnopol | 19 ± 8 | 17 ± 7 |
| Mhhp | 15 ± 2 | 11 ± 3 |

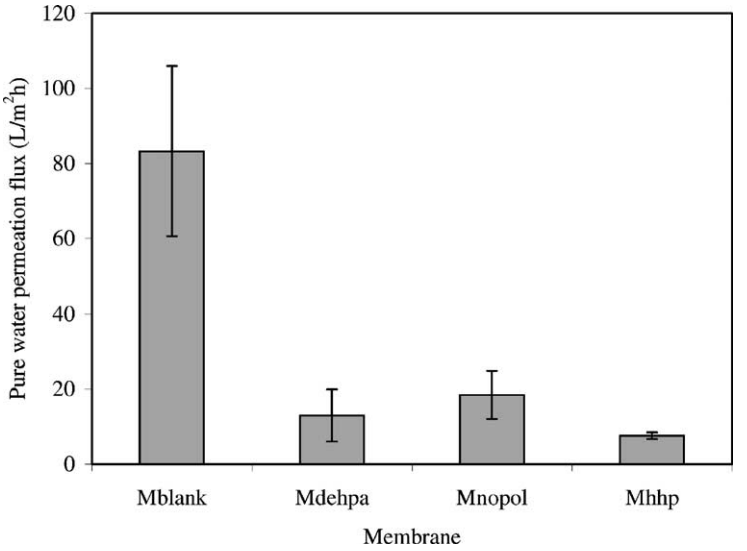


Fig. 2. Pure water permeation fluxes for the four composite membranes (error bars correspond to S.D.).

membranes. This difference between Mblank and ACMs can be explained by considering two mechanisms of mass transport, one through the pores and the other through the polymer matrix. There is practically no separation of electrolyte (from water) by the first mechanism, while the electrolyte separation will take place by the second mechanism. Probably, in the Mblank membrane the mass transport through the polymer matrix was enhanced because of the higher wettability of the membrane, as will be evidenced later on by the lower receding contact angle obtained, and the corresponding higher degree of swelling of the polymer matrix. Hence, the main contribution of the second mechanism, in the case of Mblank membrane, results in a higher electrolyte separation. The high uncertainty values determined can be attributed to the membrane surface heterogeneity.

### 4.2. Contact angle measurement

The results of the contact angle measurements are given in Table 3. According to the results, the contact angles of all membranes were less than 90°, meaning that each membrane has a hydrophilic surface. The advancing contact angles were almost the same for all membranes, within an experimental error range, except for Mdehpa that showed a significant lower value. Interestingly, the receding contact angle was almost opposite in trend, Mdehpa being the highest. As a result, the order in the contact angle hysteresis became:

Mblank > Mhhp > Mnopol > Mdehpa

This is exactly the same order as in the surface porosity given in the last column of Table 1. Most likely, the capillary force working from the membrane pore increases the resistance against the movement of the water droplet on the membrane surface, leading to the higher contact angle hysteresis [19,31]. The presence of such contact angle hysteresis values is usually expected when characterizing such rough surfaces [19]. Surface roughness values are presented below.

Table 3
Results of contact angle measurements at the surface of the four composite membranes

| Membrane | Advancing contact angle (°) | Receding contact angle (°) | Hysteresis (°) |
|---|---|---|---|
| Mblank | 79 ± 1 | 27 ± 5 | 51 ± 5 |
| Mdehpa | 63 ± 5 | 50 ± 6 | 13 ± 6 |
| Mnopol | 76 ± 5 | 38 ± 4 | 38 ± 3 |
| Mhhp | 75 ± 8 | 32 ± 5 | 43 ± 10 |

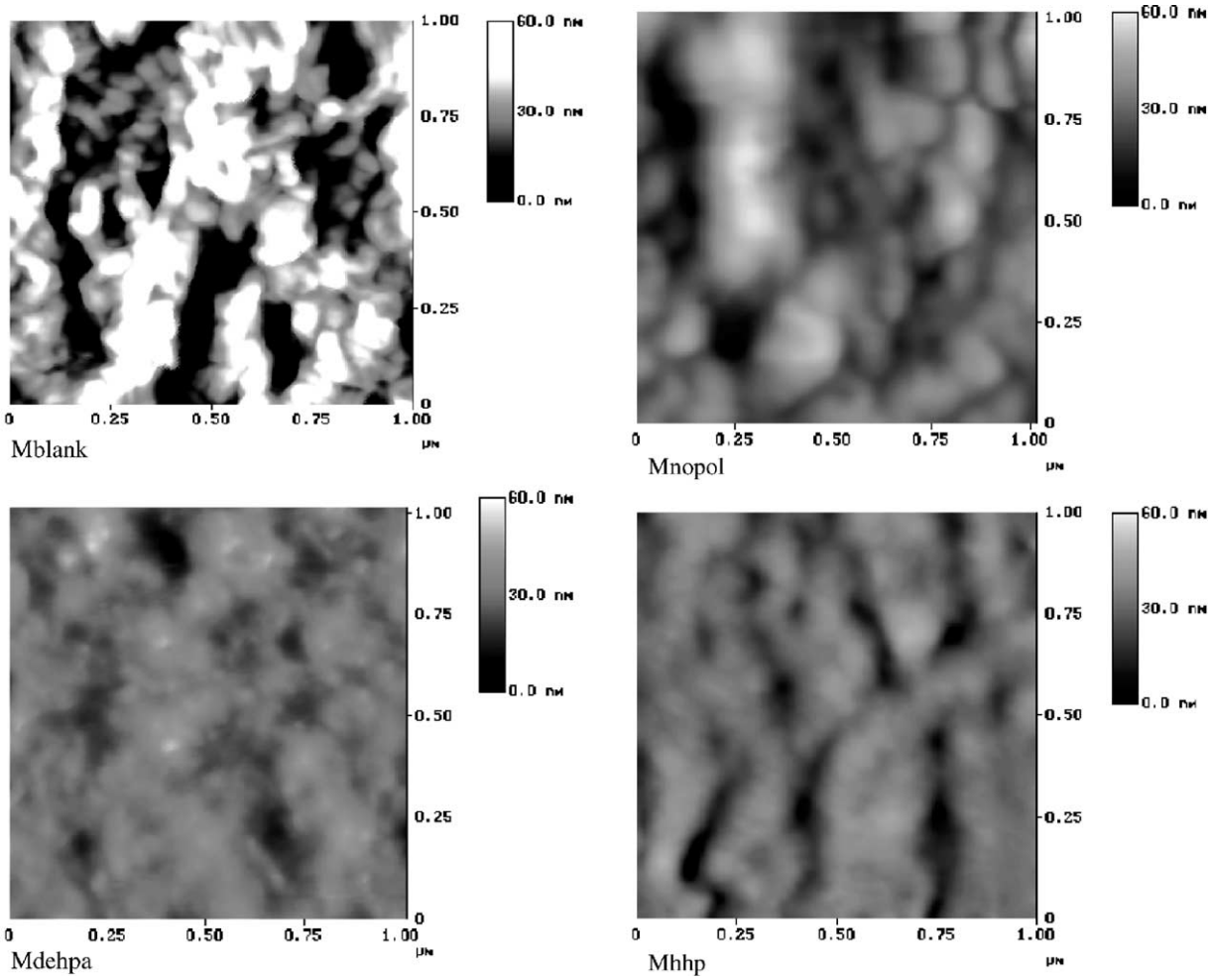


Fig. 3. Atomic force microscopy images of the top thin polyamide layer of the four composite membranes.

### 4.3. AFM measurement

The AFM images are presented in Fig. 3 for all membranes studied. The AFM parameters pertinent to these membranes are summarized in Table 4. The relatively high mean roughness values have been commonly found on the top layer of aromatic co-polyamide composite membranes [32,33]. Kwak

Table 4
Some AFM parameters obtained for the four composite membranes

| Membrane | $R_a$ (nm) | Nodule size (nm) | $\mu_p$ (nm) | $\sigma_p$ (nm) | $N$ (pores/μm$^2$) | $S_p$ (%) |
|---|---|---|---|---|---|---|
| Mblank | 14 ± 3 | 37 ± 6 | 20.11 | 1.16 | 215.7 | 7.12 |
| Mdehpa | 8 ± 4 | 37 ± 6 | 17.70 | 1.23 | 108.6 | 2.9 |
| Mnopol | 6 ± 2 | 72 ± 8 | 20.62 | 1.21 | 78.84 | 2.83 |
| Mhhp | 7 ± 2 | 36 ± 6 | 14.13 | 1.21 | 284.7 | 4.81 |

et al. [33] reported that the surface roughness is enhanced when polyamides are meta-oriented due to the presence of free amide groups that are unbound to other amide groups by hydrogen bonding as a consequence of a large intermolecular N–H···O distance. Although there is a large scatter in the values of the mean roughness, Mblank showed a value distinctively higher than ACMs. This may be attributed to the filling of depressions or pores on the surface with the carrier molecules, resulting in a smoother surface. The differences among the others ACMs are considered to be within the error range.

The nodule sizes are also given in Table 4. The nodule sizes are similar for all membranes, except for Mnopol. According to Kesting [9], these sizes correspond to macromolecular nodules. In the case of Mnopol, the obscure image did not allow measuring the size of the individual nodules; therefore the reported size seems to correspond to those of nodule aggregates. The small variation of the nodule sizes, between the membranes, can also be attributed to the presence of carriers either in the depressions or pores at the membrane surface without being fully incorporated inside the nodule. Since the interaction between the carrier and the macromolecules are thus limited, the size of the nodule is unaffected by the presence or absence of the carriers in the membrane [34].

The pore sizes measured by the AFM method are also summarized in Table 4. Compared to those listed in Table 1, the values obtained from the AFM image analysis are 2–4 times larger than those obtained from the solute transport data. A similar observation was made earlier [35]. It was argued that the pore size obtained from the solute transport data corresponds to the minimal size of the pore constriction, while the pore size obtained by the AFM method corresponds to the maximum size of the pore opening. Nevertheless, these differences may be also attributed to the uncertainty of the absolute pore dimensions measurements, due to the convolution of the tip and the nanoscale pore shapes [36]. The pore size for the Mblank membrane was again distinctively greater than ACMs, except for the pore size of Mnopol membrane, for which only an obscure surface image was obtained, as mentioned before.

Also, greater values were obtained for the pore density and surface porosity by AFM as compared with the values obtained by the method based on the solute transport. A similar observation was made earlier when the surfaces of the polyethersulfone ultrafiltration membranes were investigated [11]. This discrepancy can be attributed to two factors: on one side to some uncertainty in $\delta$ value involved in the calculation of $N$ by Eq. (5), and by the other side, to depressions of the surface without penetration through the membrane cross-section, that were mistakenly considered as pores.

### 4.4. ESR measurement

The ESR spectrum obtained from the Mblank membrane is depicted in Fig. 4 as a typical example. The spectra from the other membranes are similar to that of the Mblank membrane. The spectrum shown in Fig. 4 is considered to be an overlap of two ESR signals. One is a signal coming from the spin probe located in the pore. The motion of the spin probe is weakly restricted by the surrounding wall. The signal consists of sharp triple peaks. The other is a signal coming from the spin probe trapped inside the polymer matrix. With a strong interaction with macromolecules, the motion of the latter spin probe is strongly restricted [37]. The signal consists of triple peaks, much lower and broader than the first signal. The relative contribution from the first and second type of the spin probes can be given by the ratio of the heights of the second peak ($b$) and the first peak ($a$), called $b/a$ ratio. The greater $b/a$ ratio, the greater is the contribution from the second type of spin probe. In other words, more spins are located in the polymer matrix [17].

Table 5 summarizes the $b/a$ ratios for the studied membranes, except for Mnopol, for which was problematic to obtain a clear spectrum. The spectrum from the Mblank membrane produced a distinctively higher $b/a$ ratio. At a first glance it seems to be against

Table 5
The $b/a$ ratios obtained from ESR spectra, for the composite membranes

| Membrane | $b/a$ |
|---|---|
| Free spin probe | 1 |
| Mblank | 1.5 |
| Mdehpa | 1.1 |
| Mhhp | 1.3 |

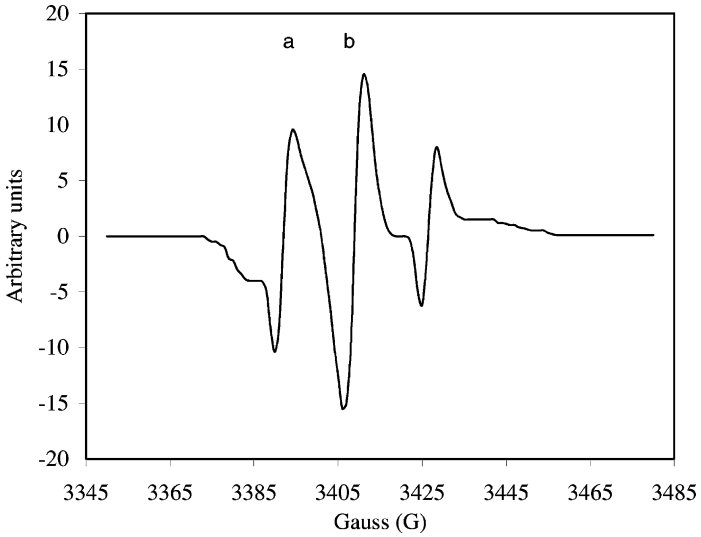


Fig. 4. ESR spectrum from the spin probe in the Mblank membrane.

expectation, since the pore size and the porosity of the Mblank membrane are greater than those of ACMs. Hence the population of radical probes in the pores of the Mblank membrane should be greater than for ACMs, leading to a lower *b*/*a* ratio. This rather conflicting observation can be explained by considering the following factors. First, the Mblank membrane is more wettable and it is swollen to a degree greater than ACMs, as evidenced by the lower receding contact angle. As a consequence, more radical probes will diffuse into the polymer matrix, increasing the number of radical probes in the polymer matrix, relative to those in the pores, thus leading to a higher *b*/*a* ratio. Second, the membranes were rinsed by distilled water before being subjected to ESR experiments, so, as the pore size is larger in the Mblank, more radical probes could be washed away during the rinsing process, increasing the effect of the first factor.

## 5. Conclusions

From the experiments conducted in this work, we may conclude that all four characterization techniques adopted here; i.e. the solute transport by ultrafiltration experiments, the contact angle measurement, the AFM and the ESR, proved to be useful tools for the characterization of ACMs.

We found that the ACMs can tolerate the cross-membrane pressure difference of 50 psig. and that they possess, unexpectedly, pores with sizes equivalent to those of ultrafiltration membranes, which are actually defects of the top dense polyamide layer.

We also can affirm that the carrier molecules were properly incorporated in the membranes, and are, most likely, located in the pores, instead of being dispersed in the polymer network of the polyamide thin layer.

These conclusions will provide an important guideline for the further improvement in the ACM design.

## Acknowledgements

T. Gumí acknowledges the *Departament d'Univesitats, Recerca i Societat de la Informació de la Generalitat de Catalunya* for the research and the travel scholarships, which made possible this work. This work has been supported by C.I.C.Y.T. (Project ref: QUI99-0794-C01). The authors are indebted with C. Feng for his contribution on the experimental design.

## References


[1] P.F.M.M. Correia, J.M.R.D. Carvalho, Recovery of chlorophenol from aqueous solutions by emulsion liquid membranes: batch experimental studies and modeling, J. Membr. Sci. 179 (1–2) (2000) 175–183.

[2] J.A. Calzado, C. Palet, M. Valiente, Metal affinity liquid membranes. Part III. Characterization of transport selectivity, J. Sep. Sci. 24 (7) (2001) 533–543.

[3] D. Stella, J.A. Calzado, A.M. Girelli, S. Canepari, R. Bucci, C. Palet, M. Valiente, Liquid Membranes for chiral separations. Application of cinchonidine as chiral carrier, J. Sep. Sci. 25 (4) (2002) 229–238.

[4] A.M. Neplenbroek, D. Bargeman, C.A. Smolders, Supported liquid membranes: instability effects, J. Membr. Sci. 67 (1992) 149.

[5] A.J.B. Kemperman, D. Bargeman, Th. Van den Boomgaard, H. Strathmann, Stability of supported liquid membranes: state of the art, Sep. Sci. Tech. 31 (20) (1996) 2733–2762.

[6] J.A. Calzado, C. Palet, M. Valiente, Facilitated transport and separation of aromatic amino acids through activated composite membranes, Anal. Chim. Acta 431 (2001) 59–67.

[7] T. Gumí, M. Oleinikova, C. Palet, M. Valiente, M. Muñoz, Facilitated transport de lead(II) and cadmium(II) through novel activated composite membranes containing di-(2-ethylhexyl)phosphoric acid as carrier, Anal. Chim. Acta 408 (2000) 65–74.

[8] M. Oleinikova, R. Garcia-Valls, M. Valiente, M. Muñoz, Procedimento para la obtención de membranas compuestas para el transporte de especies químicas, Patent 200000536.

[9] R.E. Kesting, The four tiers of structure in integrally skinned phase inversion membranes and their relevance to the various separation regimes, J. Appl. Polym. Sci. 41 (1990) 2739–2752.

[10] M. Mulder, Basic Principles of Membrane Technology, Kluwer, Dordrecht, 1992 (Chapter 4).

[11] S. Singh, K.C. Khulbe, T. Matsuura, P. Ramamurthy, Membrane characterization by solute transport and atomic force microscopy, J. Membr. Sci 142 (1998) 111–127.

[12] S. Nakao, Determination of pore size and pore size distribution. Part 3. Filtration membranes, J. Membr. Sci. 96 (1994) 131–165.

[13] A.S. Michaels, Analysis and prediction of sieving curves for ultrafiltration membranes: a universal correlation? Sep. Sci. Technol. 15 (1980) 1305–1322.

[14] G. Binnig, C.F. Quate, Ch. Gerber, Atomic force microscope, Phys. Rev. Lett. 12 (1986) 930.

[15] J.I. Calvo, P. Prádanos, A. Hernández, W.R. Bowen, N. Hilal, R.W. Lovitt, P.M. Williams, Bulk and surface characterization of composite UF membranes atomic force microscopy, gas adsorption-desorption and liquid displacements techniques, J. Membr. Sci 128 (1997) 7–21.

[16] K.C. Khulbe, T. Matsuura, Characterization of synthetic membranes by Raman spectroscopy, electron spin resonance, and atomic force microscopy; a review, Polymer 41 (2000) 1917–1935.

[17] K.C. Khulbe, T. Matsuura, G. Lamarche, A.-M. Lamarche, C. Choi, S.H. Noh, Study of the structure of asymmetric cellulose acetate membranes for reverse osmosis using electron spin resonance (ESR) method, Polymer 42 (2001) 6479–6484.

[18] I. Noda, Contact angle studies of surface-hydrophilic elastomer films, in: K.L. Mittal (Ed.), Contact Angle, Wettability and Adhesion, The Netherlands, 1993, pp. 373–381.

[19] F. Garbassi, M. Morra, E. Occhiello, Polymer Surfaces. From Physics to Technology, Wiley, New York, NY, 1994 (Chapter 4).

[20] F.-U. Hsieh, T. Matsuura, S. Sourirajan, Reverse osmosis separations of polyethylene glycols in dilute aqueous solutions using porous cellulose acetate membranes, J. Appl. Polym. Sci. 23 (1979) 561–573.

[21] M. Meireles, A. Bessieres, I. Rogissart, P. Aimar, V. Sanchez, An appropriate molecular size parameter for porous membranes calibration, J. Membr. Sci. 103 (1995) 105–115.

[22] G. Nabi, Light-scattering studies of aqueous solutions of poly (ethylene oxide), Pakistan J. Sci. 20 (1968) 136–140.

[23] F.-U. Hsieh, T. Matsuura, S. Sourirajan, Analysis of Reverse osmosis data for the system polyethylene glycol-water-cellulose acetate membrane at low operating pressures, Ind. Eng. Chem. Process Des. Dev. 18 (1979) 414–423.

[24] K.H. Youm, W.S. Kim, Prediction of intrinsic pore properties of ultrafiltration membrane by solute rejection curves: effect of operating conditions on pore properties, J. Chem. Eng. Jpn. 24 (1981) 1–7.

[25] J. Benavente, M. Oleinikova, M. Muñoz, M. Valiente, Characterization of novel activated composite membranes by impedance spectroscopy, J. Electroanal. Chem. 451 (1998) 173–180.

[26] C. Lipson, N.J. Sheth, Statistical Design and Analysis of Engineering Experiments, McGraw-Hill, New York, 1973, p. 18.

[27] M. Mulder, Basic Principles of Membrane Technology, Kluwer, Dordrecht, 1992 (Chapter 3).

[28] S. Sourirajan, T. Matsuura, Reverse Osmosis/Ultrafiltration Process Principles, National Research Council of Canada, 1985.

[29] R.J. Petersen, Composite reverse osmosis and nanofiltration membranes, J. Membr. Sci 83 (1993) 81–150.

[30] J. Benavente, A. Canyas, Transport of $NaNO_3$ solutions across an activated composite membranes: electrochemical and chemical surface characterizations, J. Membr. Sci 156 (1999) 241–250.

[31] A. Nabe, E. Staude, G. Belfort, Surface modification of polysulfone ultrafiltration membranes and fouling by BSA solutions, J. Membr. Sci 133 (1997) 57–72.

[32] S-Y. Kwak, D.W. Ihm, Use of atomic force microscopy and solid-state NMR spectroscopy to characterize structure-property-performance correlation in high-flux reverse osmosis (RO) membranes, J. Membr. Sci. 158 (1999) 143–153.

[33] S.-Y. Kwak, S.G. Jung, Y.S. Yoon, D.W. Ihm, Details of surface features in aromatic polyamide reverse osmosis membranes characterized by scanning electron and atomic

force microscopy, J. Polym. Sci. Part B Polym. Phys. 37 (1999) 1429–1440.
[34] K.C. Khulbe, G. Chowdhury, B. Kruczek, R. Vujosevic, T. Matsuura, G. Lamarche, Characterization of the PPO dense membrane prepared at different temperatures by ESR, atomic force microscope and gas permeation, J. Membr. Sci. 126 (1997) 115–122.
[35] A. Bessieres, M. Meireles, R. Coratger, J. Beauvillain, V. Sanchez, Investigations of surface properties of polymeric membranes by near field microscopy, J. Membr. Sci. 109 (1996) 271–284.
[36] W.R. Bowen, A.W. Mohammad, N. Hilal, Characterization of nanofiltration membranes for predictive purposes-use of salts, uncharged solutes and atomic force microscopy, J. Membr. Sci. 126 (1997) 91–105.
[37] R.S. Alger, Electron Paramegnetic Resonance, Interscience, New York, NY, 1968.

**ANNEX C**

# APPLICATION OF ACTIVATED COMPOSITE MEMBRANES CONTAINING THE CHIRAL CARRIER N-HEXADECYL-L-HYDROXYPROLINE FOR FILTRATION PURPOSES

Tània Gumí[1], Carles Torras[2], Ricard Garcia-Valls[2] and Cristina Palet[1,*]

[1]*Centre Grup de Tècniques de Separació en Química, Unitat de Química Analítica, Departament de Química, Universitat Autònoma de Barcelona, 08193-Bellaterra, Catalunya, Spain.*

[2] *Departament d'Enginyeria Química, ETSEQ, Universitat Rovira i Virgili, Av. Països Catalans 26, 43007-Tarragona, Catalunya, Spain.*

* Corresponding author. E-mail: Cristina.Palet@uab.es, Fax: +34935812379, Tel: +34935813475.

**Abstract**

Activated composite membranes, ACM, containing the chiral carrier N-hexadecyl-L-hydroxyproline have been tested for the propranolol filtration, and both permeation rate and enantioselectivity have been evaluated. Afterwards, the ACM have been characterized by Scanning Electron Microscopy. SEM membrane images have been further treated with IFME program, and certain morphological properties of the ACM, such as mean internal pore size, internal regularity, and internal symmetry were determined. Their morphological structure has been studied and well related with their obtention procedure. Resulting data were finally compared with the results from other characterization techniques applied previously for such membranes.

*Keywords*: Activated Composite Membranes, Filtration, Propranolol, SEM, IFME.

## 1. Introduction

Membrane separation systems have been gaining importance, in last years, as enatioresolution techniques, since they offer several advantages over traditional methods, such as; low time cost, set-up simplicity and the possibility to be used in continuous mode.

In that sense, various membrane configurations, have been already proposed for the separation of a broad number of species, including aminoacids and its derivatives, and drugs. Different liquid membrane types, based either in chiral liquids or in solutions of chiral molecules (namely chiral selectors or carriers), were firstly proposed to resolve racemic mixtures [1]. Crown ethers, polyaminoacids or cyclodextrines are some of the most widely employed chiral molecules in membrane solutions [2]. However, liquid membranes processes, when applied for the separation of enantiomers, experience a rapid decrease of selectivity, due to the free diffusion of analytes across the membranes, and additionally, they show low stability and short lifetime when tested under industrial separation conditions [3]. Therefore, solid polymeric membranes based mostly in ultrafiltration membranes [4-5] or polymer impringting membranes [6] have been developed.

For the case of SR-propranolol, a β-blocking drug used for treating certain cardiovascular anomalies (with the S-enantiomers showing far more blocking activity than the R-enantiomer [7-8]), different enantioselective carriers have been studied. On one hand, N-n-alkyl-hydroxyprolines [9-10], and dialkyl tartrate [11] were used in liquid membrane configurations. In both cases, the carrier is present in the membrane phase and selectively

forms a favored complex with one of the enantiomers, which is transported across the membrane by an ion pairing mechanism [9-10]. These transport systems are driven by a proton gradient between both feed and stripping aqueous phases. On the other hand, N-n-alkyl-hydroxyprolines have also been employed as chiral carriers in polymeric membranes [12], and chiral derivatized polysulfone [13], or norbornadiene [14], have been considered as chiral polymers.

In this work, activated composite membranes (ACMs), developed previously [15], and successfully applied for the separation of metal ions [16], or aminoacids [17], are considered for the enantioresolution of SR-propranolol with the aim of N-hexadecyl-L-hydroxyproline as carrier.

## 2. Experimental

### *2.1 Reagents*

R-propranolol hydrochloride, S-propranolol hydrochloride and racemic propranolol hydrochloride, all a. r. grade, were supplied by Sigma-Aldrich (Germany). N-hexadecyl-L-hydroxyproline (HHP), isopropyl myristate (IPM), triethanolamine and hydroxypropyl-β-cyclodextrin (HP-β-CD), all a. r. grade, were also purchased from Sigma-Aldrich (Germany). All other reagents used (such as acids and inorganic salts) were of analytical grade. MilliQ water was used for all aqueous solutions.

### *2.2 Membranes*

Polysulfone (PS) (Basf, Spain) was dissolved in a.r. grade N,N-dimethylformamide (DMF, Sigma-Aldrich) to a concentration of 15 wt.%, and the solution was cast on the surface of a non-woven fabric and, all together, immersed into a coagulation bath at ca. 4°C. Then, a thin polyamide layer was formed on the top surface of the polysulfone membrane, by in-situ interfacial polymerisation of 1,3-phenylenediamine (Merck, Germany) dissolved in water, with trimesoyl chloride dissolved in hexane (both from Sigma-Aldrich, Germany). The membranes were chemically activated by addition of the chiral carrier, either in the polysufone casting solution, or into the hexane solution used for the preparation of the top polyamide layer. The carrier HHP was firstly dissolved in IPM, previous to be added to the casting solution. More details of the membrane preparation are given elsewhere [18]. A blank membrane, without carrier, was prepared and tested for comparison. The membranes are labeled, hereafter, as ACM1 (blank membrane), ACM2 (the chiral carrier is introduced during the formation of the top PA layer) and ACM3 (the chiral carrier is introduced in the PS casting solution).

SEM images were obtained by using an scanning electronic microscope HITACHI S-570 (Hitachi LTD. Tokyo, Japan) in the UAB Microscopy Service.

*2.3 Apparatus and Procedure*

The filtration experiments were preformed by using a dead-end filtration membrane module, operating in batch mode, over a membrane area of 11.3 $cm^2$ at a constant pressure of 3.5 bar, provided by a corresponding $N_2$ flux [19]. All experiments were performed at 24 ± 1 °C and at least twice. The membrane module was filled with different

volumes of feed solution (always containing 0.1g/L of racemic propranolol and adjusted at pH 8 with borax buffer) and conveniently pressured. Feed solution was stirred during the whole experiment with the aim of an electromagnetic stirrer, just to avoid the formation of a diffusion layer attached to the membrane [18]. Experiments started when the permeation was initiated. The permeation of each enantiomer, during the filtration process, was determined by monitoring their concentration in the permeate. For this purpose, samples were periodically withdrawn over the whole experiment.

Membranes were characterized by SEM in order to study their superficial and internal morphology. Furthermore, SEM images were treated with IFME® programme, created by C. Torras *et al.*, to determine the mean internal pore size, as well as, internal membrane symmetry and regularity [20].

*2.4 SR- Propranolol Determination*

A capillary electrophoresis (CE) system (P/ACE SYSTEM MDQ, Beckman, USA) was used to analyze the concentration of both enantiomers in the collected samples. Determination was performed in 50 μm i. d. uncoated fused-silica capillaries of 60 cm (50 cm to the detector). Before each set of analyses, the capillary was rinsed with a 0.1 M NaOH solution, MilliQ water and finally with the separation buffer solution. The latter consisted of 100mM phosphoric acid adjusted at pH 4.4 with triethanolamine, containing 17.4 mM hydroxypropyl-β-cyclodextrin (HP-β-CD) [21-22]. The applied voltage was 23kV and UV detection was carried out at 210nm. Samples were injected using the hydrodynamic mode for 5s, at 0.3 psi. The capillary was thermo stated at 20ºC. Between

consecutive determinations, the capillary was rinsed with MilliQ water. At the end of the day, the capillary was washed with NaOH 0.1 M, MilliQ water and MeOH, which was used for removing organic material and water.

*2.5 Calculations*

Both, the permeation rate of racemic propranolol through the chiral activated composite membranes, and its enatioselectivity were investigated. The permeation rate is expressed in terms of permeation percentage (P), which is calculated as the ratio of S- or R-propranolol concentration in the permeate at any time t ($Cp_{t,E-}$) to the initial S- or R-propranolol concentration in the feed phase ($Cf_{0,E-}$):

$$P = (Cp_{t,E-} / Cf_{0,E-}) * 100 \quad (1)$$

The enantioselectivity of the process is given in terms of alpha values ($\alpha$). Such alpha values were calculated by the following equation [5]:

$$\alpha = (Cp_{t,S-} / Cp_{t,R}) / (Cf_{0,S-} / Cf_{0,R-}) \quad (2)$$

where $Cp_{t,S-}$ and $Cp_{t,R-}$ apply for the concentration, in the permeate, of S- and R-enantiomers of propranolol, respectively, at any time. $Cf_{0,S-}$ and $Cf_{0,R-}$ correspond to the initial feed concentration of S- and R-enantiomers, respectively.

## 3. Results and discussion

Various activated composite membranes, ACM, containing different carriers, including different kind of chiral carriers, had been prepared previously [19], and some of them were applied for the enantioseparation of racemic propranolol under dialysis conditions. However, propranolol transport across ACM was not encountered, in those cases. It was believed that, such behaviour was probably a consequence of two different factors: a deficient or null incorporation of the carrier in the ACMs and/or, the formation of a dense top PA layer, hindering species transport across the ACM. Therefore, an in-depth characterization of the membranes was carried out. The data collected gave evidences of an appropriate incorporation of the chiral carriers into the ACM [19], suggesting that the absence of propranolol transport can be related with the membrane dense properties. Thus, ACM containing the chiral carrier HHP (which resulted the most appropriated for the SR-propranolol enantioseparation) have been here prepared and tested under pressure, for filtration purposes.

*Filtration of propranolol through ACM*

Propranolol permeation throughout was here determined. Figure 1 shows the initial and steady state permeation flux values of the three ACM. The first thing to note is that the permeation flux values obtained here, for all the membranes, are much lower than permeation flux values commonly defined for filtration experiments performed at 3.5 bar, which are ranged between 170 and 1700 L/m$^2$h [18]. It is undoubtedly due to the dense PA top layer of the ACM, which considerable increase the membrane resistance to the

feed permeation. The working pressure used in this study, corresponds to ultrafiltration experiments, which are performed, as a rule, with porous membranes, instead of composited membranes. The latter, work generally under pressures of 10-60 bar. Nevertheless, the aim of this work was not the achievement of a rapid an efficient permeation flux (as it is the case of other chemical separation systems), but a selective permeation, which usually arises at low permeation rates [12]. For this reason, dense membranes and lower working pressures were combined.

Taking into consideration the huge range of permeation flux (PF) usually defined at 3.5 bar, it seems that significant differences are not encountered among the activated composite membranes. Even so, if considering the slight differences within them, it is seen that the permeation flux follows the order ACM2 > ACM3 > ACM1. From this order it can be observed that the incorporation of the carrier HHP in the membrane (case of ACM2 and ACM3) facilitates the transport of propranolol across the ACM. Besides, the highest PF is reached when the carrier is added into the PA top layer, as this is directly in contact with the feed phase. The PF values encountered, in the present case, differ significantly from the ones determined in previous studies, were blank membrane showed the higher flux [19], which was attributed to certain polymerization defects of the top PA layer. Hence, it can be stated that the polymerization of the PA layer has been, in the present case, successfully completed.

It is also important to note that in all cases the PF suffers from an initial decrease during the first hours of experiment. This permeation flux decrease is inherent of filtration experiments, and it is usually related to concentration polarization on the active membrane side [18].

The mean permeation percentage of both enantiomers of propranolol, for each membrane type, are collected in Table 1. S- and R-propranolol permeation percentages were constant along with the time of filtration experiments, and the values corresponded to the initial propranolol concentration in the feed solution. So, propranolol is not retained. Such SR-propranolol permeation ocurrs, most probably, across the nanopores which are usually present in PA dense layers [19]. According to its molecular weight (MW) of 295.8 Da, and comparing with glucose and sucrose, taken as references with MW of 180 and 342 Da, and corresponding stokes radius of 3.6 and 4.7 nm, respectively, an approximate stokes radius of ca. 4nm can be assumed for propranolol [18].

Figure 2 shows the alpha values calculated for the different experiments. Unfortunately, as can be observed, a clear enantioselective tendency was not detected, although alpha values higher than 1 were observed in certain cases. It can be due to the no retention of propranolol in the membrane under the studied conditions. The pressure applied in this system, as driving force, resulted too high to permit enantioselectivity for the system conditions here investigated [12,23]. Now, once the propranolol permeation has been proved, ACM performance, in terms of enantioselectivity may be enhanced by increasing the carrier concentration in the membrane. Investigations are now forwarded in that way.

*Characterization of ACM by SEM and IFME®*

Also, the obtained ACMs were characterized by using Scanning Electron Microscopy (SEM) in order to investigate their surface and cross-section morphological structure. Figure 3 shows the SEM images for the three ACM. As may be observed, all of them

present, as expected, the typical morphological structure of ultrafiltration membranes prepared by phase inversion technique with DMF/water as solvent/non-solvent pair, i.e.; asymmetric morphology with the presence of macrovoids [18], with an additional noteworthy dense top layer. However in the case of ACM3, the asymmetric structure is not so evident and hardly no macrovoid may be observed. Such morphological feature, can be directly related with the composition of the PS casting solution, which in this case contained the carrier HHP dissolved in IPM. The latest, IPM, acts as an extra non-solvent, approaching the differences in polarity between DMF and water. Thus, it causes a decrease of the PS precipitation rate in the coagulation bath, leading to a more symmetric structure with a lower number of macrovoids. Also from SEM images, it can be noted that the three ACM present a regular surface that confirms the existence of a top dense polyamide layer.

Figure 4 (a, b and c) and Table 2 show IFME results from SEM images of Figure 3 [20]. Both internal asymmetry and irregularity of membranes, defined as asymmetry along y or x axes, respectively, of a piece of membrane cross-section SEM images were evaluated. As may be seen in the figure, ACM1 (Figure 4a) and ACM2 (Figure 4b) show huge variation of the internal pore distribution, specially along y axes. This is a direct consequence of the presence of macrovoids. Therefore, relatively high asymmetry and irregularity values were encountered. On the other hand, in the case of ACM3 (Figure 4c) the internal pore distribution variation encountered was smoother and more linear. So, relatively low asymmetry and irregularity values are, so forth, found for this membrane (see Table 2).

As expected, ACM1 and ACM2 have similar parameter values due to the same PS layer preparation step. The PS layer occupies most part of the membrane cross-section image.

To sum up, it may be added that the morphological parameters determined in that case do not show a significant effect over membrane filtration properties.

## 4. Conclusions

Differences in morphological properties have been encountered between ACM3 and the rest (ACM1 and ACM2). Whereas the former presents a quite symmetric and regular internal structure, with a top dense layer, ACM1 and ACM2 show an asymmetric internal structure with macrovoids and a top dense layer. Permeation of propranolol throughout the three ACM was attained. Even so, clear enantioselective permeation has not been detected in any case.

## Acknowledgements

This work has been supported by C.I.C.Y.T. (Ref: PPQ2002-04267-C03-01). Tània Gumí acknowledges *el Ministerio de Educación, Cultura y Deporte*, for the pre-doctoral fellowship.

**References**

[1] J.T.F. Keurentjes, F.J.M. Voermans, Membrane Separations in the production of optically pure compounds, in A.N. Collins, G.N. Sheldrake, J. Crosby (Eds.), Chirality in Industry II. Developments in the Commercial Manufacture and Applications of Optically Active Compounds, Wiley, Chichester, UK, 1997, pp. 157-182.

[2] L.J. Brice, W.H. Pirkle, Enantioselective Transport trough Liquid Membranes, in S.Ahuja (Ed.), Chiral Separations. Applications and Technology, ACS, Washington (USA), 1997, 309-334.

[3] A.J.B. Kemperman, D. Bargeman, Th. Van den Boomgaard, H. Strathmann, Stability of Supported Liquid Membranes: State of the Art, Sep. Sci. Tech., 31 (1996) 2733-2762.

[4] T. Masawaki, M. Sasai, S. Tone, Optical Resolution of an Amino Acid by an Enantioselective Ultrafiltration Membrane, J. Chem. Eng. Japan, 25 (1992) 33-39.

[5] A. Higuchi, H. Yomogita, B.O. Yoon, T. Kojima, M. Hara, S. Maniwa, M. Sayito, Optical resolution of amino acid by ultrafiltration using recognition sites of DNA, J. Memb. Sci., 205 (2002) 203-212.

[6] M. Yoshikawa, K. Yonetani, Molecularly imprinted polymeric membranes with oligopeptide tweezers for optical resolution, Desalination, 149 (2002) 287-292.

[7] S. Ahuja, Chiral Separations and Technology: An Overview, in S. Ahuja (Ed.), Chiral Separations. Applications and Technology, ACS, Washington, DC (USA), 1997, pp. 1-7.

[8] I.M. Coelhoso, M.M. Cardoso, R.M.C. Viegas, J.G. Crespo, Modelling of Transport Mechanism in Liquid Membranes, in S.Luque, J.R. Alvarez (Eds.), Proceedings of Engineering with Membranes, Universidad de Oviedo, Oviedo, 2001, V1, pp. 425-430.

[9] C.M. Heard, J. Hadgraft, K.R. Brain, Differential facilitated transfer across a solid-supported liquid membrane, Bioseparation, 4 (1994) 111-116.

[10] T. Gumí, M. Valiente, C. Palet, Characterization of a Supported Liquid Membrane Based System for the Enantioseparation of SR-Propranolol by N-Hexadecyl-L-Hydroxyproline, Sep. Sci. Tech., 39 (2004) 431-447.

[11] J.T.F. Keurentjes, L.J.W.M. Nabuurs, E.A. Vegter, Liquid membrane technology for the separation of racemic mixtures, J. Membr. Sci., 113 (1996) 351-360.

[12] T. Gumí, M. Valiente and C. Palet, Characterization of chiral activated membranes for the enantioseparation of SR-propranolol by response surface modelling, submitted.

[13] T. Gumí, C. Minguillón and C. Palet, Characterization of membranes based in chiral derivatized polysulfone. Application to the separation of propranolol enantiomers, submitted.

[14] T. Aoki, M. Ohshima, K. Shinohara, T. Kaneko and E. Oikawa, Enantioselective permeation of racemates through a solid (+)-poly[2-[dimethyl(10-pinanyl)silil] norbornadiene] membrane, Polymer, 38 (1997) 235.

[15] M. Oleinikova, R. Garcia-Valls, M. Valiente, M. Muñoz, Procedimento para la obtención de membranas compuestas para el transporte de especies químicas, Patent 200000536.

[16] T. Gumí, M. Oleinikova, C. Palet, M. Valiente, M. Muñoz, Facilitated transport of lead(II) and cadmium(II) through novel activated composite membranes containing di-(2-ethyl-hexyl)phosphoric acid as carrier, Analytica Chimica Acta, 408 (2000) 65-74.

[17] J.A. Calzado, C. Palet, M. Valiente, Facilitated transport and separation of aromatic amino acids through activated composite membranes, Analytica Chimica Acta, 431 (2001) 59-67.

[18] M. Mulder, Basic Principles of Membrane Technology, second edition, Kluwer Academic Publishers, Dordrecht, The Netherlands, 2000.

[19] T. Gumí, M. Valiente, K.C. Khulbe, C. Palet, T. Matsuura, Characterization of activated composite membranes by solute transport, contact angle measurement, AFM and ESR, J. Membr. Sci., 212 (2003) 123-134.

[20] C. Torras, R. Garcia-Valls, Quantification of membrane morphology by interpretation of Scanning Electron Microscopy images, J. Membr. Sci., 233 (2004) 119-127.

[21] C. Pak, P.J. Marriot, P.D. Carpenter, R.G. Amiet, Enantiomeric separation of propranolol and selected metabolites by using capillary electrophoresis with hydroxypropyl-β-cyclodextrin as chiral selector, J. Chrom. A, 793 (1998) 357-364.

[22] M. Fillet, I. Bechet, P. Chiap, Ph. Hubert, J. Crommen, Enantiomeric purity determination of propranolol by cyclodextrin-modified capillary electrophoresis, J. Chrom. A, 717 (1995) 203-209.

[23] S.B. Lee, D.T. Mitchell, L. Trofin, T.K. Nevanen, H. Söderlund, C.R. Martin, Antibody-Based Bio-Nanotube Membranes for Enantiomeric Drug Separations, Science, 296 (2002) 2198-2200.

TABLE LEGENDS

Table 1. Mean value of permeation percentages of filtration experiments achieved for both propranolol enantiomers.

Table 2. Numerical values of mean internal pore size, asymmetry and irregularity of membranes, calculated by IFME.

Table 1

| | % S | % R |
|---|---|---|
| ACM1 | 93.6 (10.8) | 97.6 (12.3) |
| ACM2 | 117.3 (3) | 119.1 (3.4) |
| ACM3 | 112.5 (2.6) | 111.1 (1.7) |

Table 2

| | Mean internal pore size (μm) | Asymmetry percentage | Global irregularity |
|---|---|---|---|
| ACM1 | 2.705 (0.238) | 46 % | 0.0021 |
| ACM2 | 2.764 (0.303) | 20 % | 0.0033 |
| ACM3 | 2.798 (0.383) | 14 % | 0.0004 |

FIGURE LEGENDS

Figure 1. Initial and steady state permeation flux of filtration experiments performed with the membranes under study . Error bars correspond to standard deviation of the values.

Figure 2. Evolution of alpha values versus time, for the different composite membranes (ACM). Error bars correspond to standard deviation of the values.

Figure 3. Cross-section images of a) ACM1, b) ACM2, and c) ACM3 obtained by SEM.

Figure 4. IFME® results from a) ACM1, b) ACM2, and c) ACM3 images treatment. In all cases it is shown, from left to right, the transformed photograph of a piece of membrane cross-section SEM image, and the variations of internal pore distribution along vertical and horizontal length of the images.

Figure 1

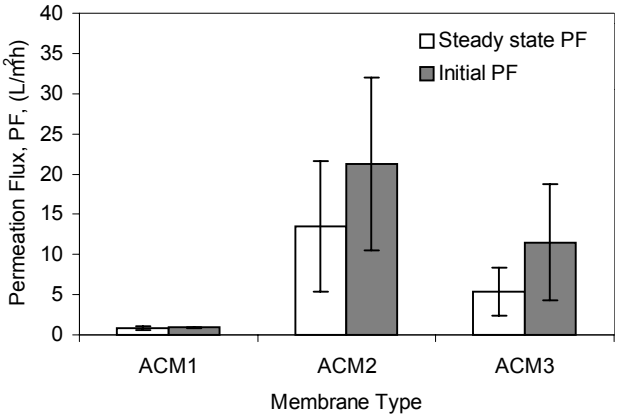
40
35
30
25
20
15
10
5
0
Permeation Flux, PF, (L/m2h)
Steady state PF
Initial PF
ACM1
ACM2
ACM3
Membrane Type

Figure 2

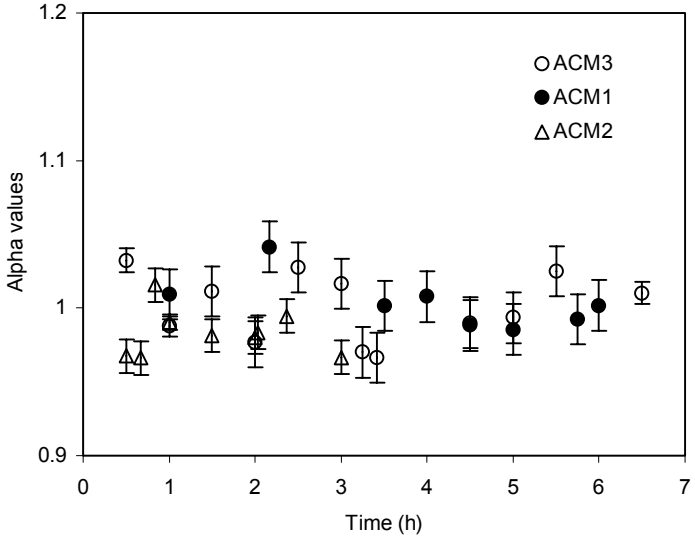

Figure 3

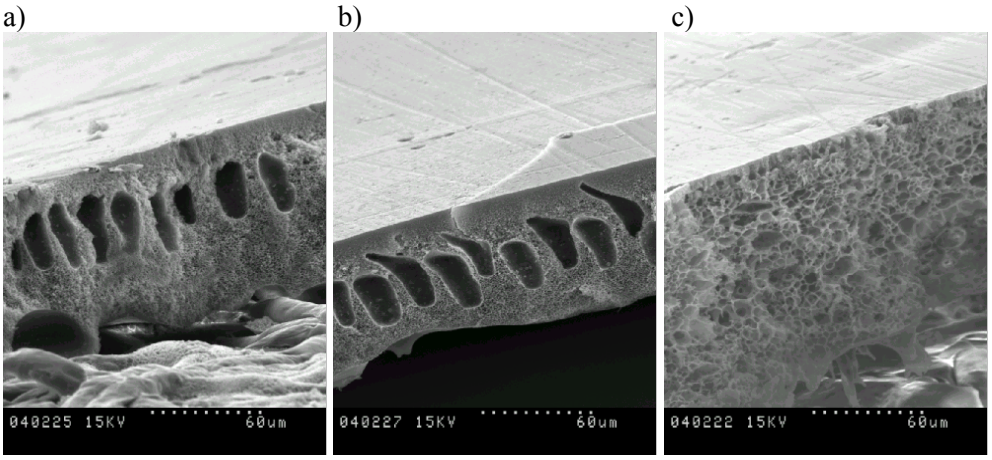

Figure 4

a)

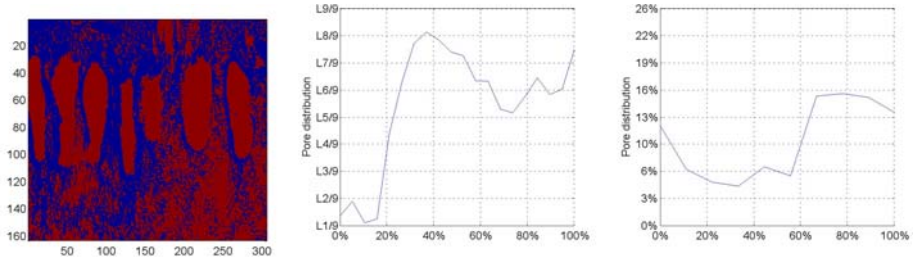
20
40
60
80
100
120
140
160
50 100 150 200 250 300
Pore distribution
L9/9
L8/9
L7/9
L6/9
L5/9
L4/9
L3/9
L2/9
L1/9
0% 20% 40% 60% 80% 100%
26%
22%
19%
16%
13%
10%
6%
3%
0%

b)

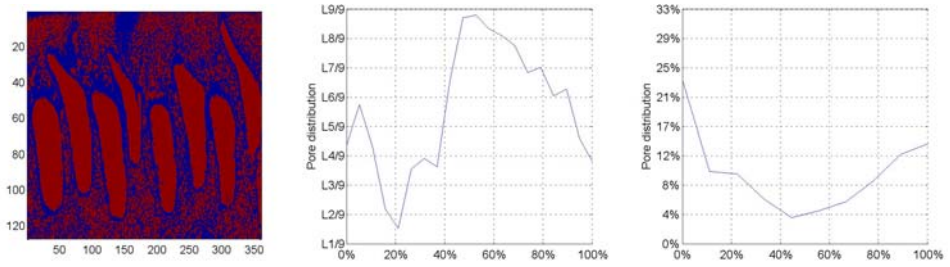
20
40
60
80
100
120
50 100 150 200 250 300 350
Pore distribution
L9/9
L8/9
L7/9
L6/9
L5/9
L4/9
L3/9
L2/9
L1/9
0% 20% 40% 60% 80% 100%
33%
29%
25%
21%
17%
12%
8%
4%
0%

c)

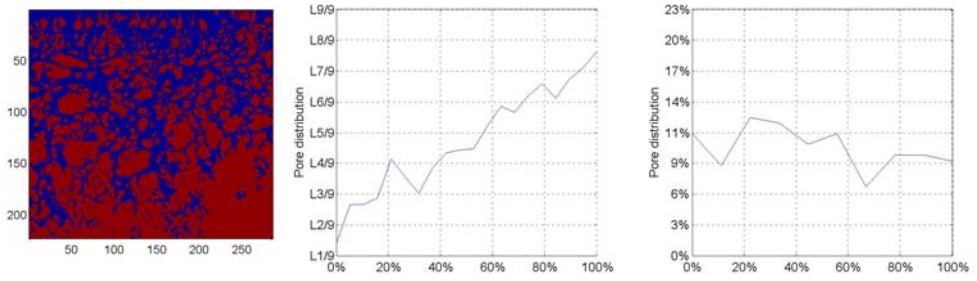
50
100
150
200
50 100 150 200 250
Pore distribution
L9/9
L8/9
L7/9
L6/9
L5/9
L4/9
L3/9
L2/9
L1/9
0% 20% 40% 60% 80% 100%
23%
20%
17%
14%
11%
9%
6%
3%
0%

**ANNEX D**

# CHARACTERIZATION OF CHIRAL ACTIVATED MEMBRANES FOR THE ENANTIOSEPARATION OF SR-PROPRANOLOL BY RESPONSE SURFACE MODELLING

T. Gumí, M. Valiente and C. Palet*

*Centre Grup de Tècniques de Separació en Química, Unitat de Química Analítica, Departament de Química, Universitat Autònoma de Barcelona, 08193-Bellaterra, Catalunya, Spain.*

* Corresponding author. E-mail: Cristina.Palet@uab.es, Fax: +34935812379, Tel: +34935813475.

**Abstract**

Chiral activated membranes have been prepared and tested for the enantioseparation of the racemic drug SR-propranolol. Polysulfone (PS) based membranes have been investigated for this purpose, and N-hexadecyl-L-hydroxyproline (HHP) has been checked as chiral carrier. The prepared membranes have been characterized by using two different membrane modules. In both cases, the concentration profile of both enantiomers of propranolol in the aqueous solutions with the time, is measured by the capillary electrophoresis technique. The influence of both, the concentration of the carrier in the membrane and the pH of the stripping solution on the membrane system have been studied by determining the propranolol transport rate (in terms of Re-extraction percentage), the corresponding separation factor (alpha) and the enantiomeric excess. Response surface modelling has been used to approach the optimum working conditions of the system (concerning stripping pH and carrier amount in the membrane) in terms of enantioselectivity. An alpha value of 1.7 has been attained.

*Keywords*: Chiral activated membranes; Enantioseparation, SR-Propranolol, Response Surface Modelling; Facilitated transport

## 1. Introduction

It is known that chirality strongly influences some chemical and biochemical reactions due to the different behaviour of the corresponding enantiomers. Meanwhile many chemical species of biological activity are prepared and used as racemic mixtures, the desired activity is often carried out by only one of the two enantiomers, while no specific activity is undertaken by the other [1]. In certain cases, the later enantiomer may inhibit the desired effect of the first enantiomer or even have adverse side effects [2]. In the case of SR-propranolol, a β-blocking drug used for treating some cardiovascular anomalies, the S-isomer shows far more blocking activity than the R-isomer [3-4]. Thus, the obtention and identification of enantiopure compounds has become one of the most important demands, specially by pharmaceutical industries, which have been forced by regulatory agencies to develop methodologies for producing pure enantiomers, in order to ensure the desired activity in the administration of drugs.

Most methods employed in the pharmaceutical industry up to date to elucidate enantiopure compounds, such as stereoselective asymmetric synthesis, biotransformation, the chiral separation processes based on the enzymatic kinetic resolution technique or diastereomeric crystallisation, have been shown to have several drawbacks. They require a considerable number of different steps, with the corresponding by-products and a high energy consumption in order to produce a reasonable amount of one optically pure enantiomer [5-7]. Certain chromatographic separations, e.g., HPLC, are even not applicable at an industrial scale. Recently, other separation processes based on chiral

stationary phases have increasingly gained attention at an industrial level, as both pure enantiomers can be obtained at the same time with far less difficulty [8]. In this context, the use of membrane technology for chiral separations offer several advantages over traditional methods; such as low time cost, set-up simplicity and relative inexpensive technology. Furthermore, when employing chiral active membranes only a small quantity of an expensive chiral selector is required [9].

Different enantioselective carriers have already been tested for the enantioseparation of RS-propranolol by using liquid membrane (LM) systems, such as N-n-alkyl-hydroxyprolines [10-11], or dialkyl tartrate [12]. In both cases, the carrier is present in the membrane phase and selectively forms a complex with one of the enantiomers, which is transported across the membrane by an ion pairing mechanism [6,10]. These transport systems are driven by a proton gradient between both feed and stripping aqueous phases.
However, liquid membranes systems have been shown to have low stability and short lifetime when tested under industrial separation conditions [13-14]. In an attempt to improve the stability and the lifetime of the liquid membranes, solid polymeric membranes, chiral activated, have been here developed. Certain solid polymeric activated membrane systems have already been proposed to resolve racemic mixtures based mostly in ultrafiltration membranes [15-16] or polymer impringting membranes [17].
In the present work, chiral activated membranes, based on polysulphone polymeric support, containing N-hexadecyl-L-hydroxyproline have been applied for the enantioselective transport of SR-propranolol. The corresponding solid chiral activated membrane system has been characterized, in terms of transport rate and enantioselectivity, by varying systematically the carrier amount in the membrane and the

stripping pH. The amount of carrier in the membrane showed to have a strong influence on the system, in the liquid membrane configuration (reported previously) [11], and the stripping pH is the driving force in proton coupled transport systems (as the membrane system involved in the present work) [6]. Response surface modelling has been used to estimate the optimum working conditions of the membrane system. In certain cases, the system under study describe a non-linear behavior upon changing one of the parameters investigated and the effects of these two parameters investigated may interact significantly. Therefore, a model that combine the effect of the two parameters (i.e. response surface modeling) is required [18-19].

Furthermore, the experimental design applied to response surface modelling permits to reduce the number of experiments to be performed to a minimum, consequently lowering the costs in terms of money and time.

## 2. Experimental

### *2.1 Reagents*

R-propranolol hydrochloride, S-propranolol hydrochloride and racemic propranolol hydrochloride, all p.a. grade, were supplied by Sigma-Aldrich (Germany). N-hexadecyl-L-hydroxyproline (HHP), isopropyl myristate (IPM), triethanolamine and hydroxypropyl-β-cyclodextrin (HP-β-CD), all p.a. grade, were also purchased from Sigma-Aldrich (Germany). All other reagents used (such as acids and inorganic salts) were of analytical grade. Doubly distilled water was used for all aqueous solutions.

*2.2 Membranes*

Polysulfone (PS) casting solution (15 % wt.) was prepared by dissolving PS (Basf) in A.R. grade N,N-dimethylformamide (DMF, Sigma-Aldrich). PS membranes were obtained by phase inversion technique of the polysulfone casting solution over a non-woven fabric, which assured re-enforced PS membranes [20]. Membranes were chiral activated by addition of different amounts (0, 0.6 or 1.2 %wt. with respect to PS) of the chiral carrier HHP, previously dissolved in IMP, in the casting solution.

*2.3 Apparatus and Procedure*

Two different membrane modules, namely module A and module B (see Figures 1a and 1b), were used.

Module A consists of two compartments (for the aqueous feed and stripping solutions) of 0.2 $dm^3$ connected by a circular window where the membrane was placed [21]. The surface area of the membrane was 12 $cm^2$. Maxon A-max (19mm) stirring motors were employed to stir the solutions at both compartments. The experiments started by switching on the stirring motors at both compartments. In each experiment, the stirring rates of both feed and stripping solutions were equal and kept constant throughout the experiment at 1200 r.p.m. [22]. The transport of each enantiomer was determined by monitoring their concentration in the feed and stripping solutions. For this purpose, samples of 0.5 ml were periodically withdrawn from both aqueous solutions over the whole experiment.

Module B was supplied by Prof. J. A. Jonsson (Lund University, Sweden). It consists of two circular PTFE blocks (diameter 120 mm and thickness 8 mm) with grooves arranged as an Archimedes' spiral (depth 0.25 mm, width 1.5 mm and length 2.5 m, with a total volume of ca. 0.95 ml). Two aluminum blocks (thickness 6 mm) were placed on both sides of the PTFE blocks in order to stabilize the construction [23]. The membrane was placed between the PTFE blocks and the whole construction was clamped tightly together with six screws. The total volume (20ml) of each aqueous phase (both the feed and the stripping) was pumped with a peristaltic pump (Minipuls 3, Gilson, France) at 0.2 ml/min flow rate, through acid-resistant tubing (Acid Manifold Tubing, Elkay Products, USA) connected to the membrane module by screw plastic FIA fittings at both PTFE disks. Both aqueous phases were circulated throughout the whole experiment. The experiments started when both feed and stripping solutions filled completely their respective channels. Samples of 0.5 ml were periodically withdrawn from feed and stripping phase channels in order to monitor the concentration of both enantiomers of propranolol. A multimagnetic stirrer (A-03, SBS, Spain) was employed to stir both aqueous phases reservoirs with the aim of supplying the membrane with homogeneous solutions. In all cases, the two solutions flowed in a counter-current mode.

All experiments were performed at 24 ± 1 °C. In all experiments, feed phase contained 0.1g/L of racemic propranolol and was adjusted at pH 8 with borax buffer. Stripping phase was buffered with disodium phosphate at various pH values (i.e. 3, 5 and 7).

*2.4 SR- Propranolol Determination*

A capillary electrophoresis (CE) system (P/ACE SYSTEM MDQ, Beckman, USA) was used to analyze the concentration of both enantiomers in the collected samples. Determination was performed in 50 μm internal diameter uncoated fused-silica capillaries of 60 cm (50 cm to the detector). Before each set of analyses, the capillary was rinsed with a 0.1 M NaOH solution, doubly distilled water and finally with the separation buffer solution. The latter consisted of 100mM phosphoric acid adjusted at pH 4.4 with triethanolamine, containing 17.4 mM hydroxypropyl-β-cyclodextrin (HP-β-CD) [24-25]. The applied voltage was 23kV and UV detection was carried out at 210nm. Samples were injected using the hydrodynamic mode for 5s, at 0.3 psi. The capillary was thermo stated at 20ºC. Between consecutive determinations, the capillary was rinsed with doubly distilled water. At the end of the day, the capillary was washed with NaOH 0.1 M, doubly distilled water and MeOH, which was used for removing organic material and for facilitating capillary drying.

*2.5 Calculations*

Both, the transport rate of the SR-propranolol through a chiral activated membrane, and the membrane enatioselectivity were investigated. The transport rate is expressed in terms of Re-extraction percentage (R), which is calculated as the ratio of S- or R-propranolol concentration in the stripping phase at any time t ($Cs_{t,E-}$) to the initial S- or R-propranolol concentration in the feed phase ($Cf_{0,E-}$):

$$R = (Cs_{t,E-} / Cf_{0,E-}) * 100 \quad (1)$$

The R values presented here correspond to the sum of the Re-extraction percentage of the two enantiomers.

The enantioselectivity of the process is given in terms of alpha values ($\alpha$) as well as in terms of enantiomeric excess (ee). Alpha values were calculated by the following formula [26]:

$$\alpha = J_{t,S-} / J_{t,R} \quad (2)$$

where $J_{t,S-}$ and $J_{t,R-}$ apply for the flux of S- and R-enantiomers of propranolol, respectively at any time. Flux is calculated as [20]:

$$J_{t,E-} = -(V*\Delta C) / (Q*\Delta t) \quad (3)$$

Where V is the volume of feed or stripping phase, $\Delta C$ is the concentration variation in the corresponding aqueous solutions at the time increment $\Delta t$ , and Q is the membrane area.

The enantiomeric exces corresponds to the ratio of the difference between the concentration of both enantiomers in the stripping phase to the total amount of both enantiomers transported at any time and was calculated by using [27]:

$$ee = [(C_{t,S-}-C_{t,R-})/(C_{t,S-}+C_{t,R-})] * 100 \quad (4)$$

Where $C_{t,S-}$ and $C_{t,R-}$ correspond to the concentration of the S-enantiomer and R-enantiomers at any time, respectively.

*2.6 Response Surface Modelling*

Response Surface Modelling was performed using Umetrics AB Modde 5.0. The chiral activated membranes were characterized by using an experimental design, based in a Full Fac (3 levels) quadratic design, adapted to the needs of the present work. The influence of the stripping pH (when maintaining all other conditions constants) on the behaviour of membrane transport systems based in a facilitated transport associated with a proton antiport, has been widely investigated [20]. Therefore, the influence of this parameter was only fully investigated for a unique HHP concentration (other than 0) in the membrane. In this sense, seven different points and corresponding replicates were assayed. Table 1 collects the values of both variables (stripping pH and HHP amount in the membrane) in each experiment performed. The system responses were modeled by a second order polynomial function as follows:

$$y_{obs} = b_o + b_1x_1 + b_2x_2 + b_{12}x_1x_2 + b_{11}x_1^2 + b_{22}x_2^2 + e \quad (5)$$

In equation (5), $b_o$ is a constant, $b_1$ and $b_2$ express the main effect of each variable, $b_{12}$ correspond to the interactive effects between the variables, $b_{11}$ and $b_{22}$ indicate whether any of the variables has a minimum or a maximum, and e correspond to the difference between the observed and the calculated response.

## 3. Results and discussion

The chiral activated membranes, prepared as mentioned above, were characterized for the enantioselective transport of SR-propranolol, by using HHP as carrier. For that purpose, the amount of carrier in the membrane and the pH of the stripping solution were varied simultaneously. Figures 2a and 2b show the influence of the variation of these two parameters on the R (Re-extraction percentatge) of both enantiomers of propranolol together across the membrane when employing membrane module A. Results are presented as response surfaces at different times (at 24h and 48h after starting the experiment for Figure 2a and 2b, respectively). Table 2 show the obtained model and regression coefficients to equation (5) from the various analysis. Good adjusts of the response surface model were obtained for both Figures 2. As may be seen, either after 24h or 48h of experiment, the transport of SR-propranolol across the membrane is only detected when the carrier HHP is present in the membrane phase. It means that the presence of the chiral carrier in the membrane facilitates the incorporation of the propranolol into the membrane phase and as a consequence, its transport to the stripping phase is also facilitated.

It can also be observed that, when HHP is incorporated in the membrane, for the same HHP concentration, the R increases when stripping pH decreases, specially at high HHP concentrations. This fact is due to the driving force existing in this transport system; the transport of propranolol from the feed phase to the stripping phase is here taking place by the ion-pair-formation with the carrier HHP and it is associated with a proton antiport

from the stripping to the feed phase. The decrease of the stripping pH enhance the driving force of the process causing an increase of the transport rate.

The amount of carrier in the membrane influences also the Re-extraction of propranolol. In that case, the higher R values were encountered when the amount of HHP in the membrane was of 0.6%, while higher amounts of carrier in the membrane lead to lower R values. High amount of carrier in the membrane can lead to denser membranes. The latter will show higher resistance to the analyte transport through itself. Although the presence of HHP in the membrane facilitates the transport of SR-Propranolol, relatively high amounts of HHP difficult it. So the amount of HHP is a critical parameter.

The enantioselectivity of the membrane system is presented in Figure 3 in terms of alpha (3a) as well as in terms of enantiomeric excess (3b) as response surfaces.

As seen, alpha values higher than 1 and enantiomeric excess (ee) over 0 are only encountered when working at stripping pH 7 and with the highest HHP amount in the membrane (1,2%). These conditions correspond to the experiment having the slowest propranolol transport rate. As expected [28], enantioselectivity was found to increase when decreasing the transport rate. Comparing with Figures 2, where re-extraction values are presented, the model adjusts (see Table 2) in the case of Figure 3a and 3b are a bit worst than for the previous cases, specially in the case of $Q^2$ (model prediction). It can be due to the fact that the enantioselectivity of these chiral systems depends principally on the transport rate instead of the parameters investigated as variables (stripping pH and HHP concentration).

Figure 4 (a and b) shows the evolution of the alpha and enantiomeric excess along with time, respectively. Both the alpha values and the enantiomeric excess decrease along with time due to the non-selective free diffusion occurring after 48 h of starting the

experiment, which tends to equal the concentration between the two enantiomers in both aqueous phases. During the first 48h of experiment the amount of S-propranolol encountered in the stripping phase was always larger than that of R-propranolol, meaning that the S-enantiomer of propranolol is transported enantioselectively across the membrane to the stripping phase. So, the stripping solution is enriched in the S-enantiomer and consequently, the feed solution is enriched in the R-enantiomer. Thus, the free diffusion of the R-enantiomer from the feed to the stripping solution is favored due to its higher concentration gradient between both aqueous phases, until reaching the racemic composition in the stripping phase.

Considering that propranolol transport is not detected through blank membranes (during the first 50h), a facilitated transport mechanism [20], driven by a pH gradient is stated. It suggests that the S-enantiomer has more affinity for the carrier HHP than the R-enantiomer. This affirmation is in contradiction with the literature, which state that the carrier HHP showed higher affinity for the R-enantiomer [10]. However, after further investigation it may be seen that the contradiction is not such. Heard et al. [10] worked with a liquid membrane configuration and found that the R-propranolol was transported in larger amount than the S-enantiomer in presence of HHP in the membrane. The transport of propranolol through liquid membranes, facilitated or not, is much faster than that through solid membranes, which offer a notable higher resistance [20]. Whereas in the present solid membrane configuration the addition of the selective carrier HHP in the membrane facilitates the transport of the enantiomer with more affinity for the carrier, the addition of the same carrier in the liquid membrane configuration may actually act as a transport retardant for the more selective enantiomer. Further investigation is conducted at present in this sense.

Membrane module B was employed in order to evaluate the influence of the membrane area to the feed phase volume ratio, the solute to carrier ratio and the role of the aqueous phases recirculation was also checked. The influence of the variation of both the amount of carrier in the membrane and the stripping pH was also checked, by simultaneously varying both parameters. Their influence on the Re-extraction of both enantiomers of propranolol across the membrane is presented in Figure 5. The corresponding surface response obtained for the propranolol Re-extraction has the same shape than for module A (see Figure 2) and was also well adjusted (model data is collected in Table 2). However the absolute Re-extraction values are in all cases higher. This may be related with the fact of using a higher membrane area to aqueous phase volume ratio together with the continuous re-circulation of the feed and the stripping solutions, which enhances the hydrodynamics comparing with module A. The decreased solute to carrier ratio in comparison with module A ($S/C_A \cong 10 * S/C_B$) also helps to the R increase.

With module B, a trans-membrane osmotic pressure was found to condition the propranolol transport across the membrane in absence of carrier. Transport of water from the feed to the stripping solution was detected, which did not occur when the ionic strength was kept equal at both aqueous phases (parameter that was also investigated in that case). On the contrary, when carrier was present in the membrane phase, the transport of propranolol through the membranes was unaffected by adjusting or not the ionic strength between feed and stripping phases, probably due to a clearly denser membranes [29].

Enantioselective transport was not detected (or when detected, it showed high uncertainty) with this membrane module, as may be seen in Figures 6 a and b. Actually, lower or unappreciable ennatioselectivity was already expected due to the relatively high transport rate values obtained. As mentioned above, when relatively high transport rates are attained, a decrease on enantioselectivity is found.

Experiments with the presence of only one of the propranolol enatiomers in the initial feed solution were also performed using membrane module A, and no difference in their transport rate was encountered. We believe that only the competence between them leads to certain enantioselectivity. That suggest that the carrier, HHP, has solely a light stronger affinity for one of the enantiomers, and therefore the enantioselectivity encountered in this system, when working with membrane module A, has more to do with the kinetics rather than with the thermodynamics differences between both enantiomers [26].

**4. Conclusions**

Response surface modelling results appropriate to study the chiral membrane system proposed and allows approaching the optimum working conditions in terms of Re-extraction percentatge (R), and consequently in terms of enantioselectivity, with good model correlations.

The pH of the stripping phase influences both the analyte transport rate and alpha values, either by using membrane module A or B. An increase in the stripping pH causes a decrease of the Re-extraction and, on the contrary, an enhancement of alpha values is found. So, enantioselectivity increases at low transport rates, as expected.

The amount of the carrier HHP incorporated in the membrane also affects the transport rate and the alpha values. In this case, HHP amounts over 0.6% in the membrane leads to lower transport rates and higher alpha values.

Higher flux values are encountered when working with membrane module B, that is related to some characteristics of this module configuration: its hydrodynamic conditions, its higher ratio of membrane area to aqueous phase volume, and the lower solute to carrier ratio tested. Therefore, better alpha values are detected when employing the membrane module A, in the periods here checked, because of the lower transport rates attained.

The presence or absence of the carrier into the membrane influences the parameters of study. In this sense, the presence of carrier in the membrane, in the case of module A, permits the analyte transport across the membrane, whereas in absence of carrier the analyte transport is detected only after 50h of experiment, and it is due to its free diffusion. In the case of membrane module B, the absence of the carrier in the membrane strongly determine the experiment performance due to the trans-membrane osmotic pressure encountered.

When working with module A at stripping pH of 7 and with membranes containing 1.2 % wt. of HHP, an alpha value of 1.67 ± 0.17 has been obtained. This configuration corresponds to the best enantioselectivity conditions.

**Acknowledgements**

This work has been supported by C.I.C.Y.T. (Ref: PPQ2002-04267-C03-01). Tània Gumí acknowledges *el Ministerio de Educación, Cultura y Deporte*, for the pre-doctoral fellowship received. The authors acknowledge Prof. J. Havel for his contribution on the experimental design.

**Referencees**

[1] H.M. Krieg, J.C. Bretenbach, K. Keiser, Chiral resolution by β-cyclodextrin polymer-impregnated ceramic membranes, J. Membr. Sci., 164 (2000) 177-185.

[2] X. Wang, X.J. Wang, C.B. Ching, Solubility, Metastable Zone Width, and Racemic Characterization of Propranolol Hydrochloride, Chirality, 14 (2002) 318-324.

[3] S. Ahuja, Chiral Separations and Technology: An Overview, in S. Ahuja (Ed.), Chiral Separations. Applications and Technology, ACS, Washington, DC (USA), 1997, pp. 1-7.

[4] I.M. Coelhoso, M.M. Cardoso, R.M.C. Viegas, J.G. Crespo, Modelling of Transport Mechanism in Liquid Membranes, in S.Luque, J.R. Alvarez (Eds.), Proceedings of Engineering with Membranes, Universidad de Oviedo, Oviedo, 2001, V1, pp. 425-430.

[5] D.W. Armstrong, H.L. Jin, Enrichment of Enantiomers and Other Isomers with Aqueous Liquid Membranes Containing Cyclodextrin Carriers, Anal. Chem., 59 (1987) 2237-2241.

[6] J.T.F. Keurentjes, F.J.M. Voermans, Membrane Separations in the production of optically pure compounds, in A.N. Collins, G.N. Sheldrake, J. Crosby (Eds.), Chirality in Industry II. Developments in the Commercial Manufacture and Applications of Optically Active Compounds, Wiley, Chichester, UK, 1997, pp. 157-182.

[7] Y. Gao, R.M. Hanson, J.M. Klunder, S.Y. Ko, H. Masamune, K.B. Sharpless, Catalytic asymmetric epoxidation and kinetic resolution: modified procedures including in situ derivatization, J. Am. Chem. Soc., 109 (1987) 5765-5780.

[8] E.R. Francotte, Enantioselective chromatography as a powerful alternative for the preparation of drug enantiomers. J. Chrom. A, 906 (2001) 379-397.

[9] P. Dzygiel, P. Wieczorek, J.A. Jonsson, M. Milewska, P. Kafarski, Separation of Amino Acid Enantiomers using Supported Liquid Membrane Extraction with Chiral Phosphates and Phosphonates, Tetrahedron 55 (1999) 9923-9932.

[10] C.M. Heard, J. Hadgraft, K.R. Brain, Differential facilitated transfer across a solid-supported liquid membrane, Bioseparation, 4 (1994) 111-116.

[11] T. Gumí, M. Valiente, C. Palet, Characterization of a Supported Liquid Membrane Based System for the Enantioseparation of SR-Propranolol by N-Hexadecyl-L-Hydroxyproline, Sep. Sci. Tech., in press.

[12] J.T.F. Keurentjes, L.J.W.M. Nabuurs, E.A. Vegter, Liquid membrane technology for the separation of racemic mixtures, J. Membr. Sci., 113 (1996) 351-360.

[13]. A.M. Neplenbroek, D. Bargeman, C.A. Smolders, Supported liquid membranes: instability effects, J. Membr. Sci., 67 (1992) 121-132.

[14] A.J.B. Kemperman, D. Bargeman, Th. Van den Boomgaard, H. Strathmann, Stability of Supported Liquid Membranes: State of the Art, Sep. Sci. Tech., 31 (1996) 2733-2762.

[15] T. Masawaki, M. Sasai, S. Tone, Optical Resolution of an Amino Acid by an Enantioselective Ultrafiltration Membrane, J. Chem. Eng. Japan, 25 (1992) 33-39.

[16] A. Higuchi, H. Yomogita, B.O. Yoon, T. Kojima, M. Hara, S. Maniwa, M. Sayito, Optical resolution of amoni acid by ultrafiltration using recognition sites of DNA, J. Memb. Sci., 205 (2002) 203-212.

[17] M. Yoshikawa, K. YOnetani, Molecularly imprinted polymeric membranes with oligopeptide tweezers for optical resolution, Desalination, 149 (2002) 287-292.

[18] M. Andersson, P. Adlercreutz, Evaluation of simple enzyme kinetics by response surface modelling, Biothecnology Techniques, 13 (1999) 903-907.

[19] S.L.R-. Ellison, D.G. Holcombe, M. Burns, Response surface modelling and kinetic studies for the experimental estimation of measurement uncertainty in derivatisation, Analyst, 126 (2001) 199-210.

[20] M. Mulder, Basic Principles of Membrane Technology, second edition, Kluwer Academic Publishers, Dordrecht, The Netherlands, 2000.

[21] C. Palet, M. Muñoz, S. Daunert, L-. Bachas, M. Valiente, Vitamin B12 derivatives as anion carriers in transport through supported liquid membranes and correlation with their behavior in ion-selective electrodes, Anal. Chem., 65 (1993) 1533-1536.

[22] R. Garcia-Valls, M. Muñoz, M. Valiente, Selective separation of lanthanides by supported liquid membranes containing Cyanex 925 as a carrier, Anal. Chim. Acta, 387 (1999) 77-84.

[23] J.A. Calzado, C. Palet, J.A. Jonson, M. Valiente, Metal affinity liquid membrane II. Facilitated transport of tryptophan, Anal. Chim. Acta, 417 (2000) 159-167.

[24] C. Pak, P.J. Marrito, P.D. Carpenter, R.G. Amiet, Enantiomeric separation of propranolol and selected metabolites by using capillary electrophoresis with hydroxypropyl-β-cyclodextrin as chiral selector, J. Chrom. A, 793 (1998) 357-364.

[25] M. Fillet, I. Bechet, P. Chiap, Ph. Hubert, J. Crommen, Enantiomeric purity determination of propranolol by cyclodextrin-modified capillary electrophoresis, J. Chrom. A, 717 (1995) 203-209.

[26] H.M. Krieg, J. Lotter, K. Keizer, J.C. Breytenbach, Enrichment of chlortalidone enantiomers by an aqueous bulk liquid membrane containing β-cyclodextrine, J. Membr. Sci., 167 (2000) 33-45.

[27] D. Stella, J.A. Calzado, S. Canepari, A.M. Girelli, R. Bucci, C. Palet, M. Valiente, Liquid membranes for chiral separations. Application of cinchonidine as a chiral carrier, J. Sep. Sci., 25 (2002) 229-238.

[28] S.B. Lee, D.T. Mitchell, L. Trofin, T.K. Nevanen, H. Söderlund, C.R. Martin, Antibody-Based Bio-Nanotube Membranes for Enantiomeric Drug Separations, Science, 296 (2002) 2198-2200.

[29] T. Gumí, M. Valiente, K.C. Khulbe, C. Palet, T. Matsuura, Characterization of activated composite membranes by solute transport, contact angle measurement, AFM and ESR, J. Membr. Sci., 212 (2003) 123-134.

Table 1. Layout of the variable settings for the experiments performed

| Experiment number | Stripping pH (1) | HHP Conc. (%) (2) | Replicates |
|---|---|---|---|
| 1 | 3 | 0 | 1 |
| 2 | 5 | 0 | 1 |
| 3 | 7 | 0 | 1 |
| 4 | 5 | 0.6 | 1 |
| 5 | 3 | 1,2 | 1 |
| 6 | 5 | 1.2 | 0 |
| 7 | 7 | 1.2 | 1 |

Table 2. Obtained model and regression coefficients to equation (5) from the analysis of table 1 for each case investigated.

| Parameter | Figure 2a | Figure 2b | Figure 3a | Figure 3b | Figure 5 |
|---|---|---|---|---|---|
| $b_o$ | 40.8 (2.5) | 85.9 (3.0) | 1 (0,05) | 3.5 (1.4) | 99.8 (6.5) |
| b1 | -6.1 (1.0) | -9.6 (1.2) | 0.12 (0.03) | 4.9 (1.5) | -10.5 (2.7) |
| $b_2$ | 14.2 (1.1) | 27.5 (1.3) | 0.12 (0.03) | 4.2 (1.5) | 21.6 (2.8) |
| $b_{12}$ | -6.3 (1.0) | -9.8 (1.2) | 0.13 (0.03) | 5 (1.4) | -9.5 (2.6) |
| $b_{11}$ | --- | --- | 0.1 (0.04) | --- | --- |
| $b_{22}$ | -28.6 (2.4) | -63.3 (3.0) | --- | --- | -44.4 (5.6) |
| $r^2$ | 0.976 | 0,990 | 0.888 | 0.784 | 0.932 |
| $Q^2$ | 0.850 | 0.930 | 0.319 | 0.328 | 0.646 |

FIGURE LEGENDS

Figure 1a. Schematics of membrane module A.

Figure 1b. Schematics of membrane module B.

Figure 2a. Response surface of SR-Propranolol re-extraction, vs. HHP concentration and stripping pH, after 24h of starting the experiments. The experiments were performed by using membrane module A.

Figure 2b. Response surface of SR-Propranolol re-extraction, vs. HHP concentration and stripping pH, after 48h of starting the experiments. The experiments were performed by using membrane module A.

Figure 3a. Response surface of alpha values, vs. HHP concentration and stripping pH, after 48h of starting the experiments. The experiments were performed by using membrane module A.

Figure 3b. Response surface of enantiomeric excess values, vs. HHP concentration and stripping pH, after 48h of starting the experiments. The experiments were performed by using membrane module A.

Figure 4a. Evolution of alpha values along with time (from experiment numbers 4, 5 and 7 listed in Table 1). The experiments were performed by using membrane module A.

Figure 4b. Evolution of enatiomeric excess along with time (from experiment numbers 4, 5 and 7 listed in Table 1). The experiments were performed by using membrane module A.

Figure 5. Response surface of SR-Propranolol re-extraction, vs. HHP concentration and stripping pH, after 23h of starting the experiments. The experiments were performed by using membrane module B.

Figure 6a. Evolution of alpha values along with time (from experiment numbers 4, 5 and 7 listed in Table 1). The experiments were performed by using membrane module B.

Figure 6b. Evolution of enatiomeric excess along with time (from experiment numbers 4, 5 and 7 listed in Table 1). The experiments were performed by using membrane module B.

Figure 1a

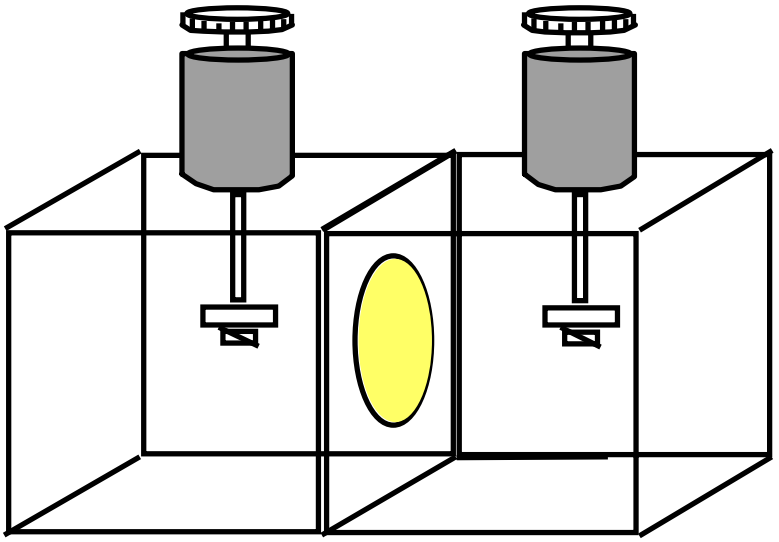

Figure 1b

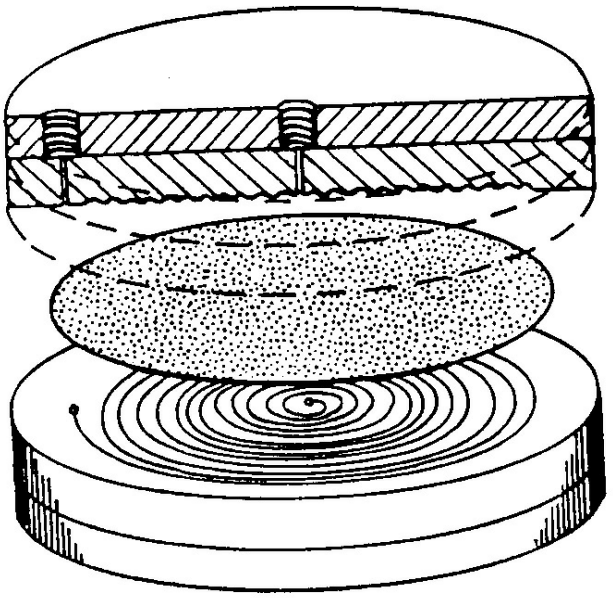

Figure 2a

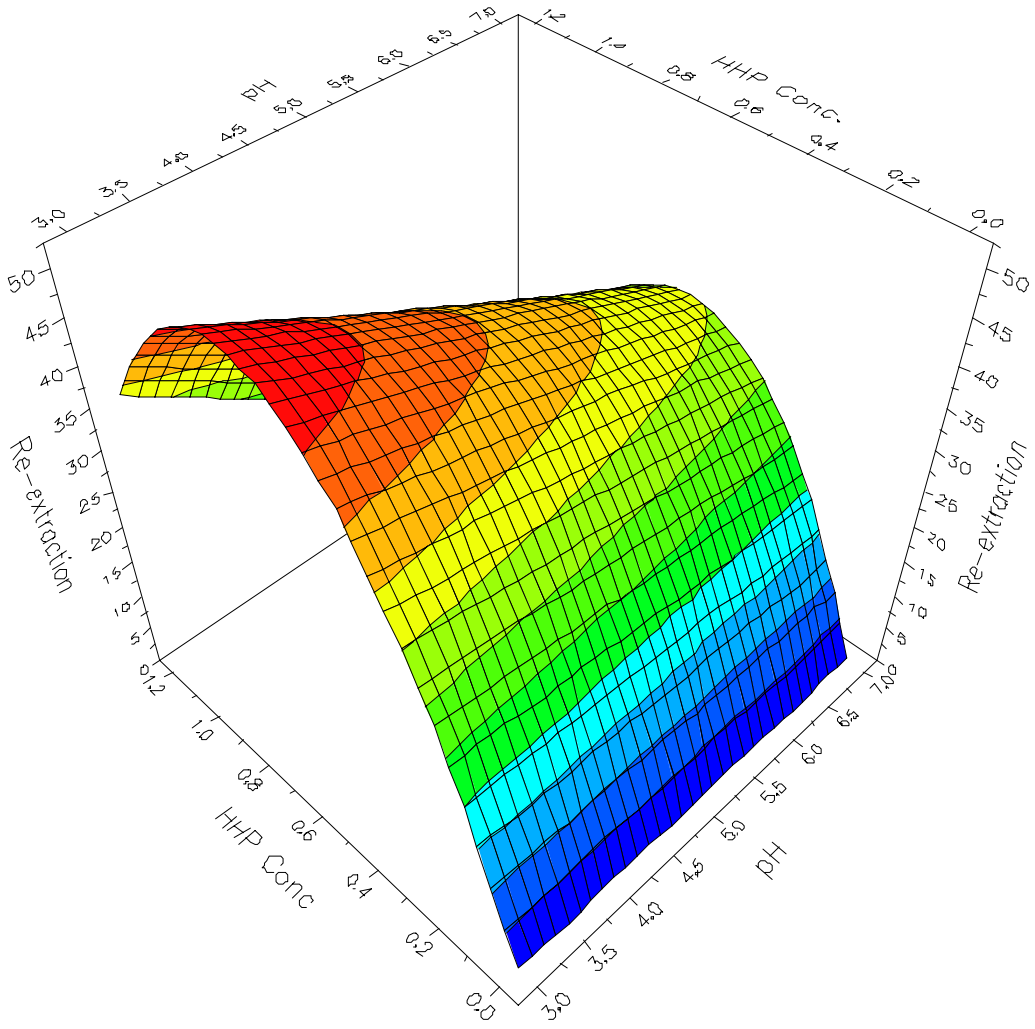

Figure 2b

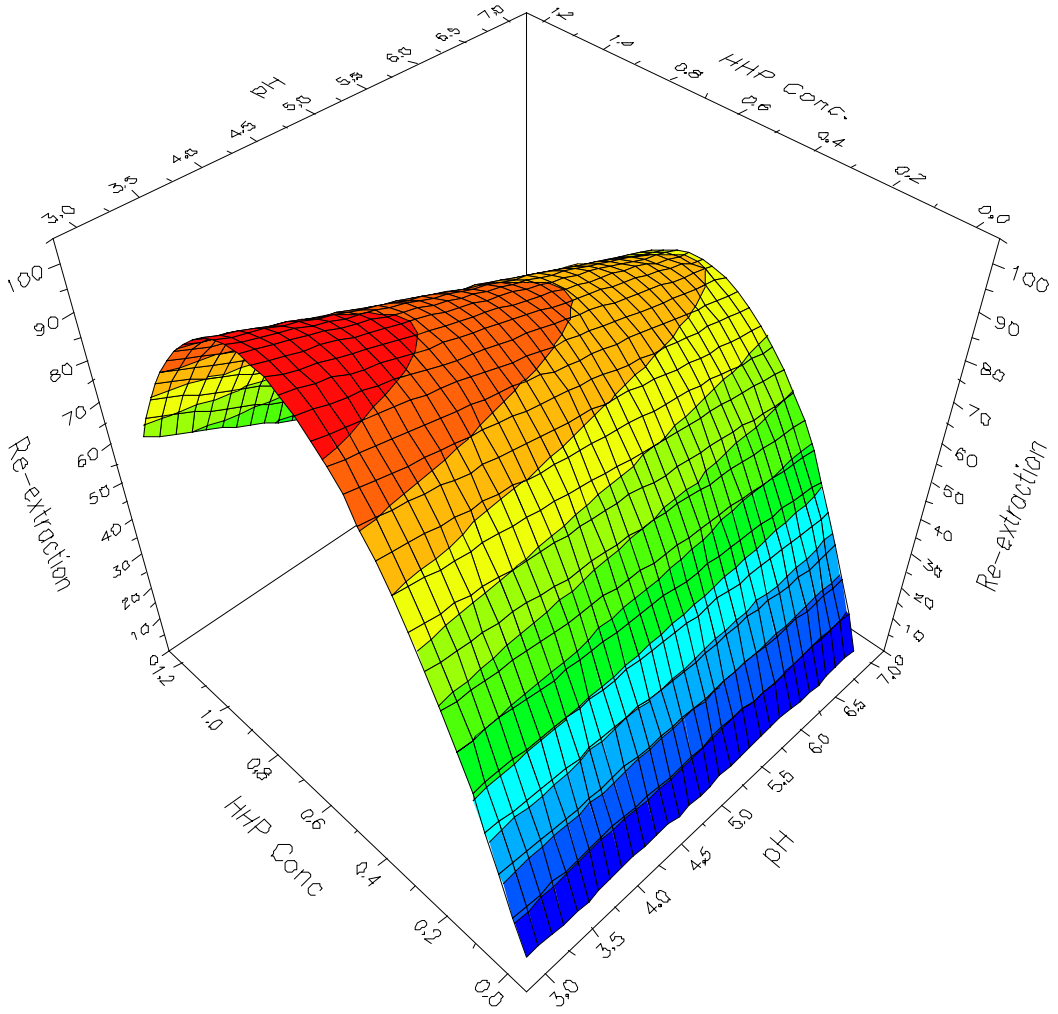

Figure 3a

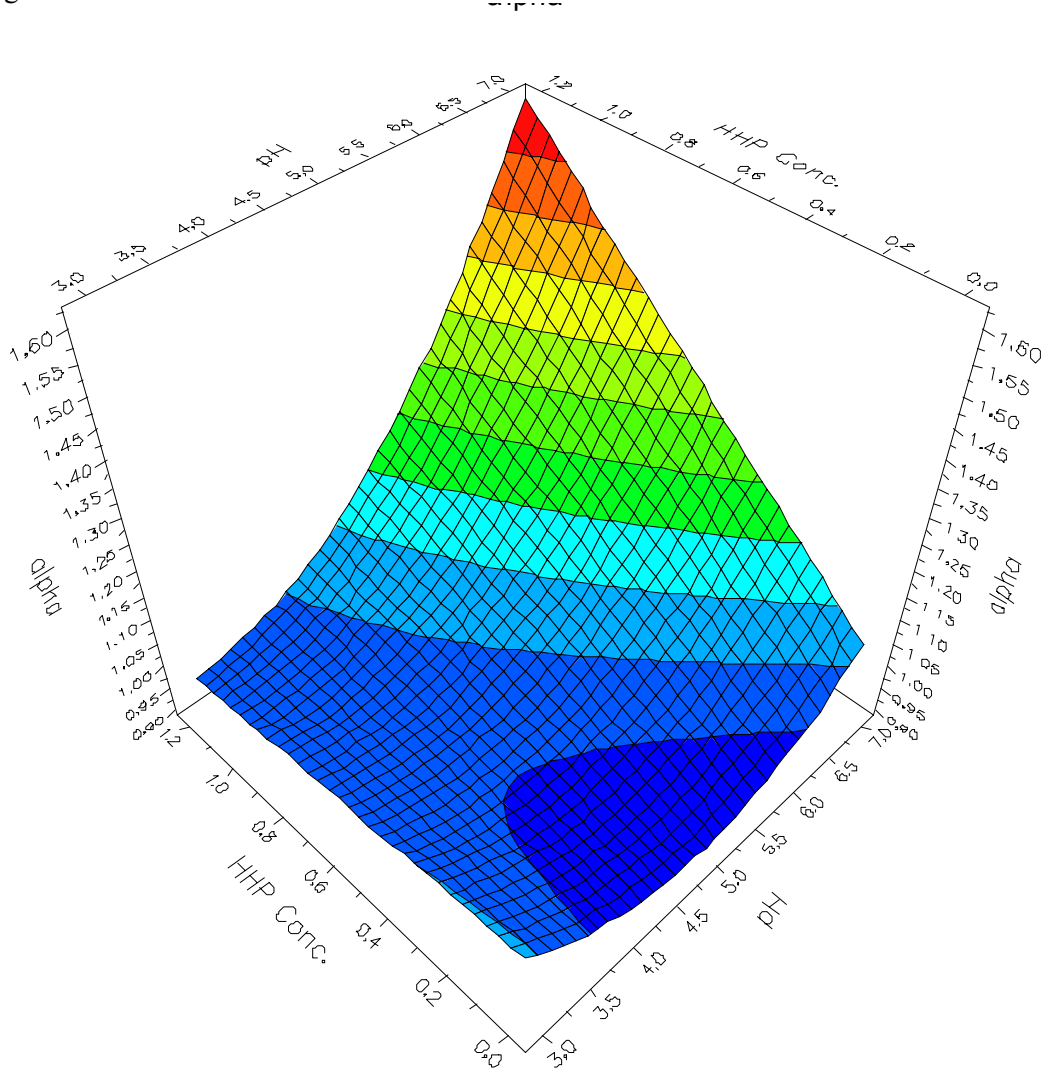

Figure 3b

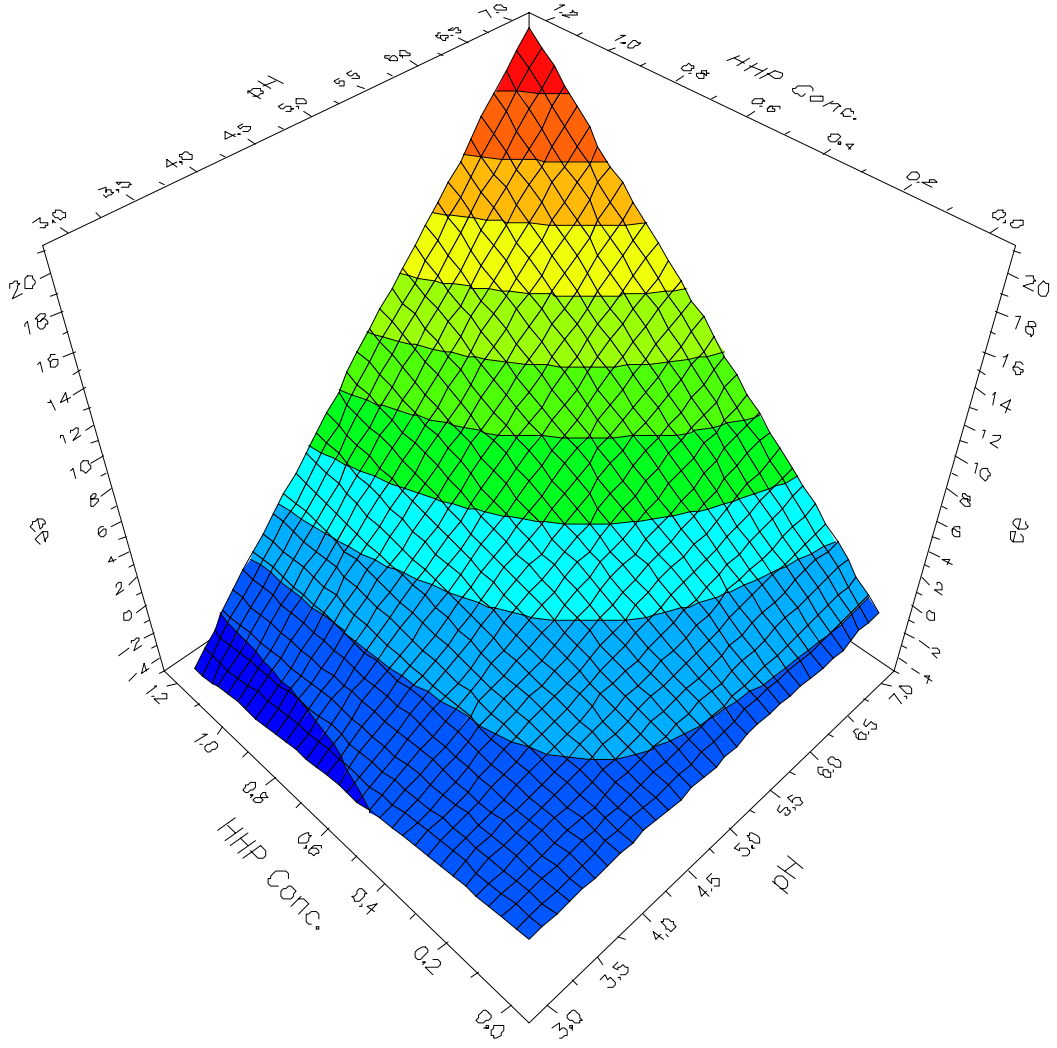

Figure 4a

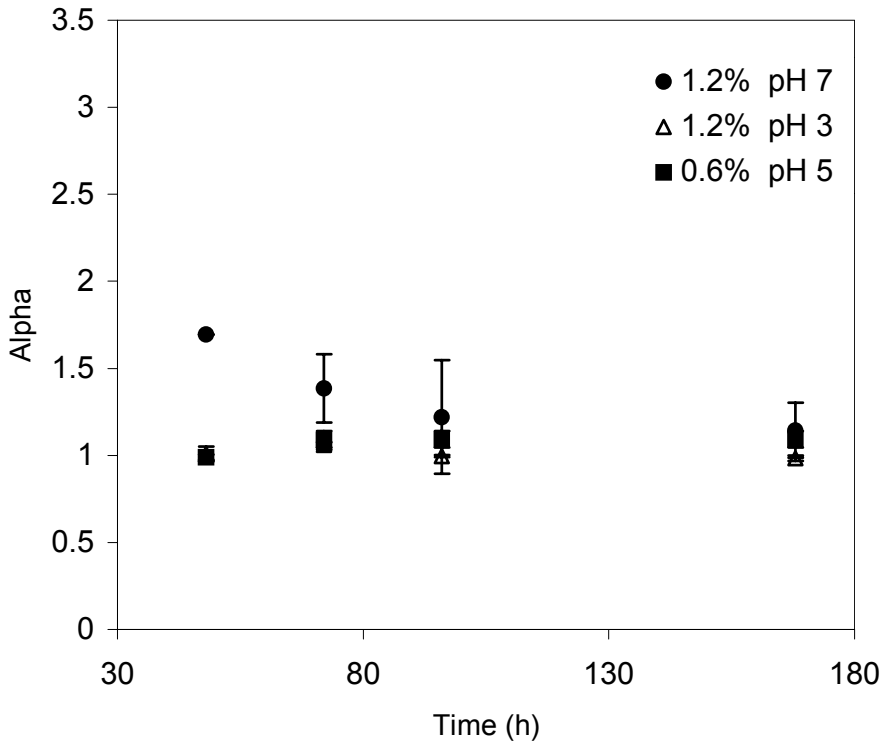

Figure 4b

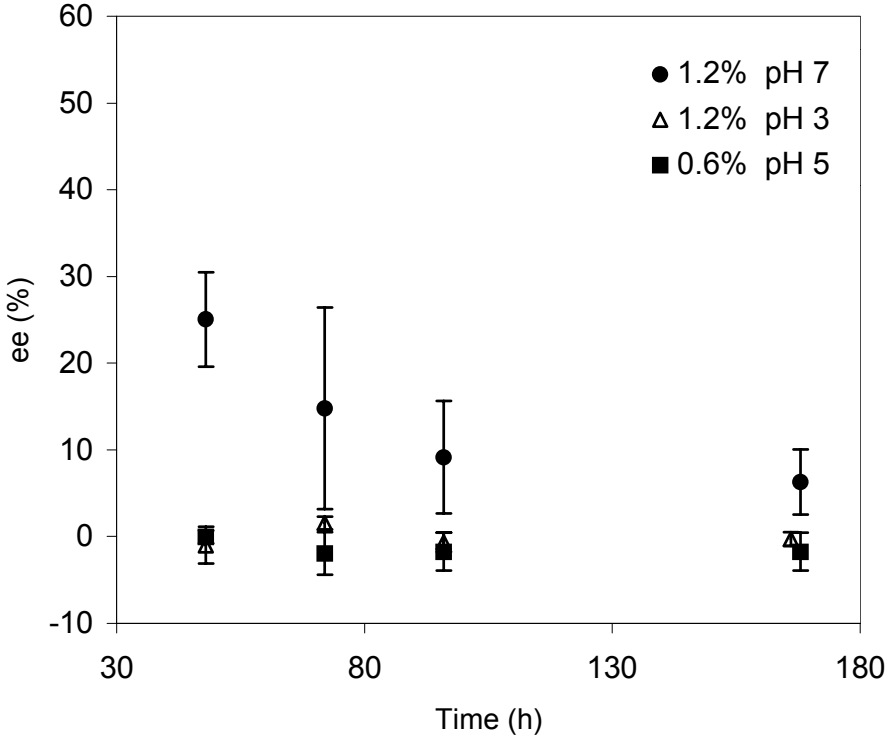

Figure 5

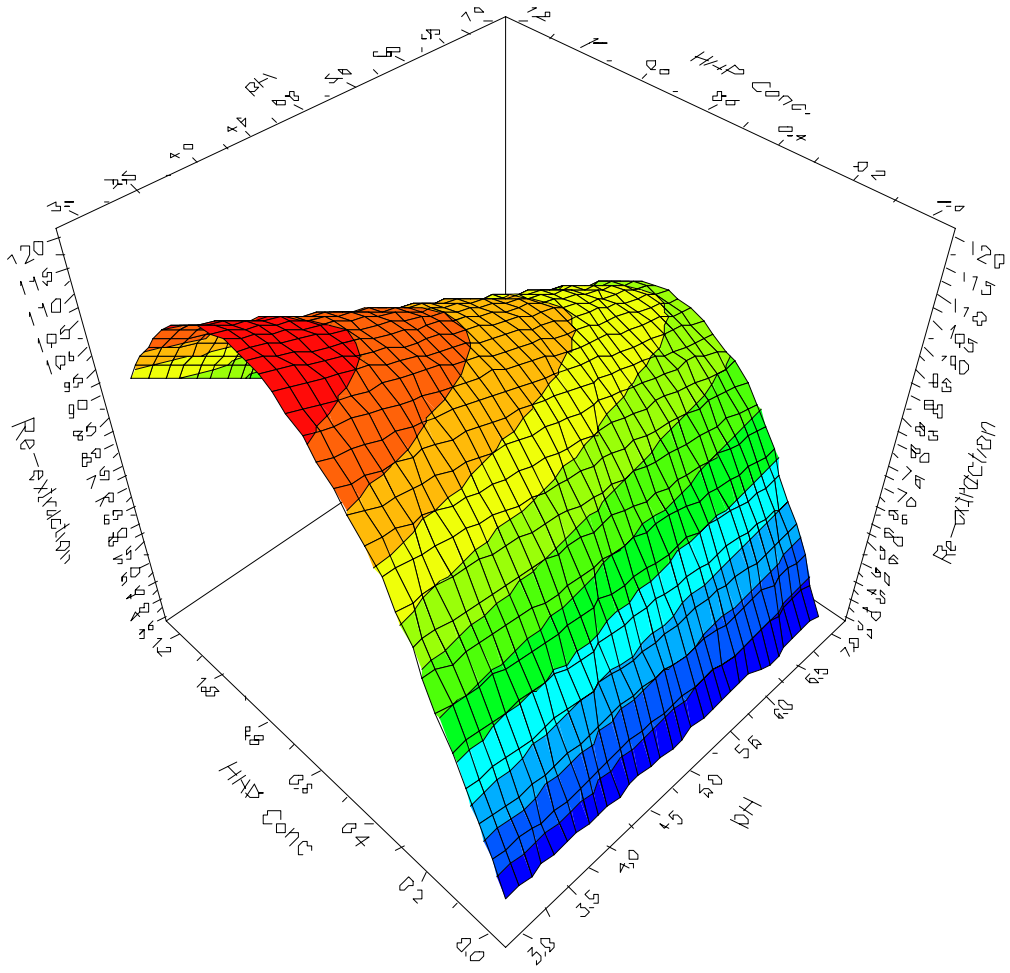

Figure 6a

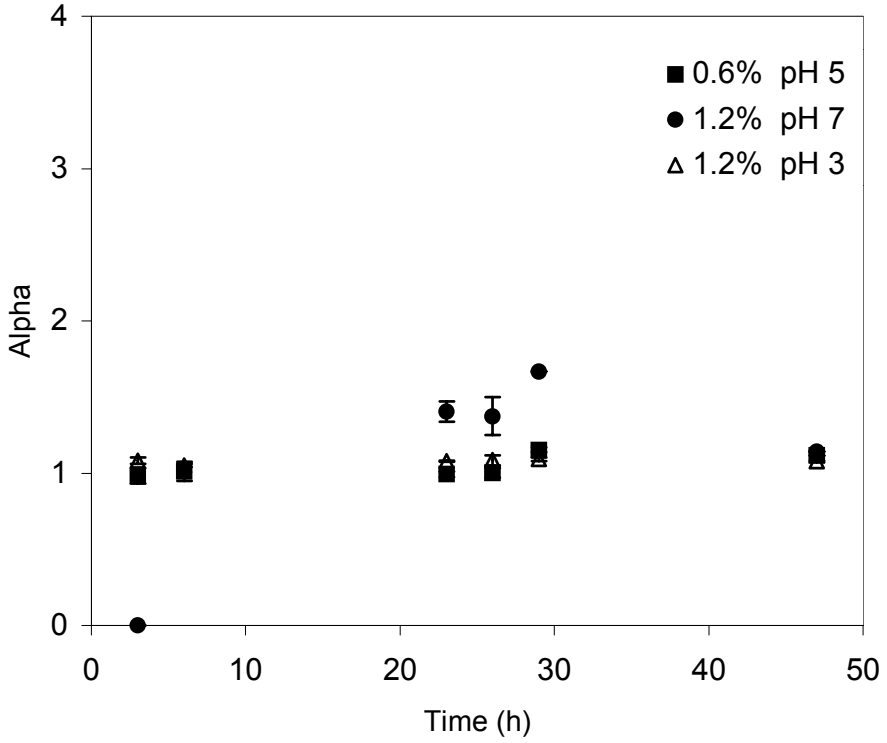

Figure 6b

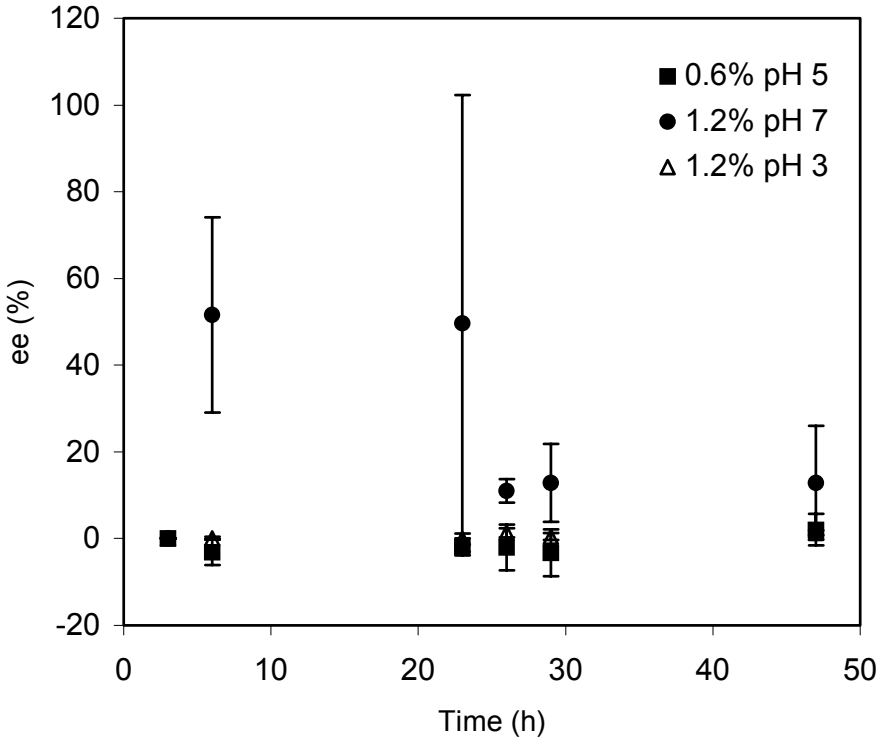
120
100
80
60
40
20
0
-20
ee (%)
0
10
20
30
40
50
Time (h)
0.6% pH 5
1.2% pH 7
1.2% pH 3